A study of ^{24}Mg by inelastic electron scattering

1974 J. Phys. A: Math. Nucl. Gen. 7 898

(http://iopscience.iop.org/0301-0015/7/8/004)

J. Phys. A: Math., Nucl. Gen., Vol. 7, No. 8, 1974. Printed in Great Britain. © 1974

A study of ^{24}Mg by inelastic electron scattering

A Johnston and T E Drake†
Kelvin Laboratory, University of Glasgow, Glasgow, Scotland

Received 20 December 1973

Abstract. The excited states of ^{24}Mg with excitation energies less than 14·0 MeV were studied by inelastic electron scattering in the momentum transfer range 0·4 to 1·14 fm^{-1}. Ground state transition probabilities and transition radii were deduced for 9 known levels with excitation less than 11 MeV and evidence was obtained for a (2^+, 4^+) doublet at 10·352 ± 0·024 MeV. In the excitation energy region 11·0 to 14·0 MeV three E2 and four E3 transitions were observed and their ground state widths were deduced. The known 2^- states at 12·67 MeV and 13·37 MeV were found to have ground state widths of $(1·4 \pm 0·5) \times 10^{-2}$ eV and $(4·0 \pm 1·4) \times 10^{-2}$ eV respectively. The form factors obtained for the low-lying states were compared with the predictions of the classical alpha particle model, the Nilsson model and Hartree–Fock calculations. Comparisons were also made with the single-particle shell model predictions for the states at 9·97, 10·70, 12·67 and 13·37 MeV.

1. Introduction

The scattering of high energy electrons from nuclei is a very valuable source of information on the spectroscopy of the target nucleus. The spins and parities of excited states may be determined and measurements made of the reduced matrix elements for nuclear transitions. In addition, however, the ability to vary the momentum transferred to the nucleus independent of the excitation energy of the nuclear state under investigation allows information to be obtained on the radial dependence of the transition matrix elements. This facility then enables detailed comparisons of experimental results with the radial dependence predicted by nuclear models.

The low-lying collective states of ^{24}Mg have been studied in several previous electron scattering experiments (Helm 1956, Titze 1969, Junk 1970, Nakada and Torizuka 1972), but the higher states, with excitation energies up to 11 MeV, have only been observed (Titze 1969) at low momentum transfer ($q < 0·6$ fm^{-1}). The present work was undertaken to extend these measurements up to $q = 1·1$ fm^{-1} and to compare the results with several nuclear models. In addition, the (e, e′) experiment of Fagg *et al* (1970) at a scattering angle of 180° presented evidence for the existence of $T = 1$, $J^{\pi} = 2^-$ states in the vicinity of 13·0 MeV excitation energy. Since no measurements in this excitation region at conventional angles exist, the present work covers the complete region 0·0–14·0 MeV.

Since this is the first extensive paper on inelastic electron scattering from this laboratory a brief description of the formalism (§ 2) and data analysis techniques (§ 4) used is presented for future reference. The experimental details are described in § 3. The results for the spectroscopic parameters of the states of ^{24}Mg are given in § 5 together with the results of other measurements. A comparison of these results with the predictions of several nuclear models is presented in § 6.

† Present address: Department of Physics, University of Toronto, Toronto, Canada.

2. The theory of electron scattering

2.1. The cross section in plane wave Born approximation

The cross section for the scattering of an electron with wavenumber $\boldsymbol{k}_i$ through an angle θ by a nucleus of charge Ze may be written (de Forest and Walecka 1966) in first order plane wave Born approximation (PWBA) as

$$\frac{d\sigma}{d\Omega} = \sigma_M \eta \left(F_C^2(q) + \frac{V_t(\theta)}{V_l(\theta)} (F_e^2(q) + F_m^2(q)) \right) \tag{1}$$

where σ_M is the Mott cross section for the scattering of high energy electrons from a heavy point nucleus and is given by

$$\sigma_M = \frac{Z^2\alpha^2}{4k_i^2} \frac{\cos^2\frac{1}{2}\theta}{\sin^4\frac{1}{2}\theta}.$$

In equation (1) η is the recoil correction factor which takes into account the finite mass of the nucleus. F_C, F_e and F_m are, respectively, the Coulomb or longitudinal, transverse electric and transverse magnetic form factors which contain all the nuclear structure information. The form factors are functions of q, the momentum transferred to the nucleus in the collision, and are related to the reduced matrix elements of the multipole operators. For example, the Coulomb form factor is given by

$$F_C^2(q) = \frac{4\pi}{Z^2}(2J_i + 1)^{-1} \sum_{L=0}^{\infty} |\langle J_f \| M_L^C(q) \| J_i \rangle|^2 \tag{2}$$

where $|J_i\rangle$ and $|J_f\rangle$ are the initial and final nuclear states respectively and $M_L^C(q)$ is the Coulomb operator given by de Forest and Walecka (1966). Similar expressions relate the transverse form factors to the matrix elements of the transverse electric and transverse magnetic multipole operators.

To a very good approximation the angular dependent term in equation (1) is given by

$$\frac{V_t(\theta)}{V_l(\theta)} = \tfrac{1}{2} + \tan^2 \tfrac{1}{2}\theta.$$

Thus the longitudinal and transverse form factors may be separated experimentally by observing the cross section for the excitation of a given nuclear state at various angles, while varying the incident energy to keep the momentum transfer constant. The variation of the form factor with momentum transfer enables the determination of the multipolarity of the transition, and this, in conjunction with the above measurement of the longitudinal or transverse nature of the state, determines the spin and parity of the final state if $J_i = 0$.

The reduced electromagnetic transition probabilities may be expressed in terms of the electron scattering form factors evaluated at $q = \omega$, where ω is the excitation energy of the state. Thus

$$B(EL\uparrow) = \frac{Z^2}{4\pi} \frac{[(2L+1)!!]^2}{\omega^{2L}} F_C^2(q = \omega)$$

for electric transitions, and

$$B(\mathrm{M}L\uparrow) = \frac{Z^2}{4\pi}\frac{[(2L+1)!!]^2}{\omega^{2L}}\frac{L}{L+1}F_{\mathrm{m}}^2(q=\omega)$$

for magnetic transitions.

2.2. *Nuclear models*

There are two aspects which arise in the analysis of an electron scattering experiment, the determination of spectroscopic information, for example the RMS radius in an elastic scattering experiment or the reduced transition probability of a state excited in an inelastic experiment, and the direct comparison of the observed cross sections with the predictions of microscopic nuclear models. The latter will be discussed in § 6. In order to obtain the spectroscopic data it is necessary to consider phenomenological nuclear models except when the experiment is carried out at very low momentum transfer. Two such models have been used in the analysis of the present experiment, namely, the Tassie model (Tassie 1956) and the Helm model (Helm 1956) as generalized by Rosen *et al* (1967).

2.2.1. Tassie model. The hydrodynamical model of the nucleus proposed by Tassie is a modification of the liquid drop model and allows non-uniform charge and mass density distributions. The nucleus in its ground state is considered to be a charged drop with a diffuse surface, with spherically symmetric charge density $\rho_0(r)$. Excited states of the nucleus are then due to oscillations of the shape of the nucleus and are described as a summation of this ground state density and a time dependent part.

One can expand the transition charge, current, and magnetization densities in terms of spherical harmonics; thus

$$\rho_{\mathrm{fi}} = \sum_{\lambda,\mu} \rho_\lambda(r) Y^*_{\lambda\mu}(\Omega)$$

$$\boldsymbol{j}_{\mathrm{fi}} = \sum_{\lambda,\lambda',\mu} I_{\lambda,\lambda'}(r) \boldsymbol{Y}^*_{\lambda,\lambda',\mu}(\Omega)$$

$$\boldsymbol{\mu}_{\mathrm{fi}} = \sum_{\lambda,\lambda',\mu} K_{\lambda,\lambda'}(r) \boldsymbol{Y}^*_{\lambda,\lambda',\mu}(\Omega).$$

In the Tassie model the various densities are given by

$$\rho_\lambda(r) = r^{\lambda-1}\,\partial\rho_0(r)/\partial r$$

$$I_{\lambda,\lambda-1}(r) = -\mathrm{i}\omega[(2\lambda+1)/\lambda]r^{\lambda-1}\rho_0(r)$$

$$I_{\lambda,\lambda}(r) = \partial\rho_0(r)/\partial r$$

$$I_{\lambda,\lambda+1}(r) = K_{\lambda,\lambda'}(r) = 0.$$

The ground state charge density used in the present analysis was the two-parameter Fermi distribution, given by

$$\rho_0(r) = \rho_0\left[1+\exp\left(\frac{(r-c)}{t/4{\cdot}4}\right)\right]^{-1}$$

where c is the half-density radius and t is the skin thickness. It has become customary to allow c and t to vary as free parameters in fitting the data for a given transition and as such will be denoted by c_{tr} and t_{tr}. The remaining free parameter is the reduced transition probability.

2.2.2. The generalized Helm model. The phenomenological model of Helm (1956) was proposed to describe the Coulomb excitation of nuclei by electrons at forward angles. It has been generalized by Rosen *et al* (1967) to provide a description of the transverse excitations observed at backward angles.

The model assumes that the transition charge, current and magnetization densities are concentrated at the nuclear surface, radius R, but are smeared out by a gaussian convolution of halfwidth g. The results for the matrix elements which enter the form factors, defined as in equation (2), are given by Rosen *et al* (1967). Two parameters define the strength of an electric transition; β_L arises from the transition charge density and γ_L^0 from the transition magnetization density. For magnetic transitions the Bessel functions $j_{L+1}(q\bar{R})$ and $j_{L-1}(q\bar{R})$ occur in the form factor expression and the corresponding strength parameters are γ_L^+ and γ_L^-. Both terms are derived from the transition magnetization density. Note that a different nuclear radius $\bar{R}$ and smearing factor $\bar{g}$ enter the results for the transverse strengths since the magnetization density is based on the matter distribution rather than the proton distribution.

3. Experimental details

3.1. Apparatus

The experiment was performed using the 120 MeV electron linear accelerator and electron scattering facility of the Kelvin Laboratory of the University of Glasgow. The equipment has been fully described elsewhere (Hogg *et al* 1972) and only a brief account is presented here.

The accelerator provides useful electron beams with energies between 20 MeV and 120 MeV with a duty cycle of about $10^{-3}\ s^{-1}$ and optimum energy resolution of 1%. Energy selection and resolution improvement are provided by a system of two 45° deflection magnets in conjunction with a pair of movable high power slit jaws. An NMR probe monitors the magnetic field. The beam produced by this system, typically 3 μA at 0·1% resolution, is focused onto a target giving a spot size of about 1 mm diameter. Current monitoring is carried out using a secondary emission monitor with frequent calibrations against a Faraday cup.

The electron detector, consisting of an array of 16 plastic (NE102) scintillators plus a Čerenkov backing detector, is mounted in the focal plane of a magic angle spectrometer (Penner 1961) with a central orbit radius of 80 cm. Field monitoring is carried out using a rotating coil gaussmeter, with 0·01% accuracy, which was calibrated using five known energies of the excited states of ^{12}C. Each detector has an intrinsic resolution of 0·1% and their centres are separated by 0·155%. The relative detector efficiencies were determined by moving the entire detector in small steps across the radiation tail of ^{12}C elastic peak, thus obtaining individual curves for each detector. Normalization to a chosen standard then provides the efficiencies.

The target used in the present experiment was a self-supporting metal foil enriched to 99·9% in ^{24}Mg and of thickness $50{\cdot}7 \pm 1{\cdot}0$ mg cm^{-2}. Uniformity measurements over the central region showed deviations in thickness of less than 3%. (The target was provided by Oak Ridge National Laboratory, Tennessee.)

3.2. *Study of* ^{24}*Mg*

Inelastic scattering spectra for ^{24}Mg were observed for 10 different combinations of energy and angle, although not all of them contain data from 0·0–14·0 MeV. Table 1 lists the energy, angle of scatter and elastic momentum transfer for each run. The entire inelastic spectrum up to 14·0 MeV was studied at momentum transfer values of 0·62, 0·80 and 0·97 fm^{-1}. Separation of the longitudinal and transverse form factors for the levels excited was obtained at $q = 0{\cdot}8$ fm^{-1} and $q = 0{\cdot}97$ fm^{-1} by repeating the measurements at backward angles. The levels below 9·5 MeV were found to be longitudinal apart from the small Siegert contribution, and a further point on the cross section curve was obtained at $q = 0{\cdot}72$ fm^{-1}, $\theta = 80°$. Several magnetic transitions occur, however, in the region 9·5–14·0 MeV and these were studied at 0·64 and 0·72 fm^{-1} at a backward angle. The region 12·0–14·0 MeV contained levels thought to have $J^{\pi} = 2^{-}$ and, therefore, excited by M2 transitions. For this reason the run at $\theta = 153°$ and $q = 1{\cdot}135$ fm^{-1} was carried out. One low momentum transfer point was obtained for the 1·37 MeV $J^{\pi} = 2^{+}$ level, at $q = 0{\cdot}39$ fm^{-1} and $\theta = 65°$.

Table 1. Kinematics of the experimental runs.

Run Number	Energy (MeV)	Angle (deg)	q_{EL} (fm^{-1})
1	91·50	120·0	0·80
2	81·66	154·0	0·80
3	110·82	120·0	0·97
4	99·21	153·0	0·97
5	64·94	154·0	0·64
6	70·92	120·0	0·62
7	73·81	153·0	0·72
8	110·07	80·0	0·72
9	115·67	153·0	1·14
10	72·6	65·0	0·40

The main features of the ^{24}Mg spectrum can be seen in figure 1(*a*) and 1(*b*) where the inelastic spectrum obtained at $E_i = 91{\cdot}5$ MeV, $\theta = 120°$ is shown. The levels below 10 MeV are clearly resolved and they include the $J^{\pi} = 2^{+}$ member of the ground state rotational band at 1·37 MeV, the 2^{+} and 4^{+} members of the $K = 2$ band at 4·23 MeV and 6·00 MeV respectively, two strong 3^{-} levels at 7·6 and 8·36 MeV, and the first excited 0^{+} state at 6·44 MeV. Above 10 MeV the spectrum becomes complex but many cross sections may be determined from lineshape analysis.

The procedure adopted in data collection was as follows. Data from the 16 detectors spanning 2·2% in momentum were accumulated followed by 3 more runs at field settings separated by $\frac{1}{4}\Delta B$, where ΔB represents the percentage detector spacing (ie 0·155%). Thus 64 points, equally spaced, were obtained spanning a 2·3% momentum bin. This method of data collection was useful in minimizing the effects of spectrometer rescattering (Hogg *et al* 1972). The rescattered spectrum does not change significantly when the field is adjusted by such small amounts and, therefore, the observed spectrum over the 2·3% energy bin is a smooth background, due to both radiation tail and rescattering, plus the narrow peaks due to inelastic scattering from excited nuclear states.

During the inelastic data accumulation repeated checks were made on the position and area of the elastic peak, and also on the efficiency of the SEM. The statistical accuracy

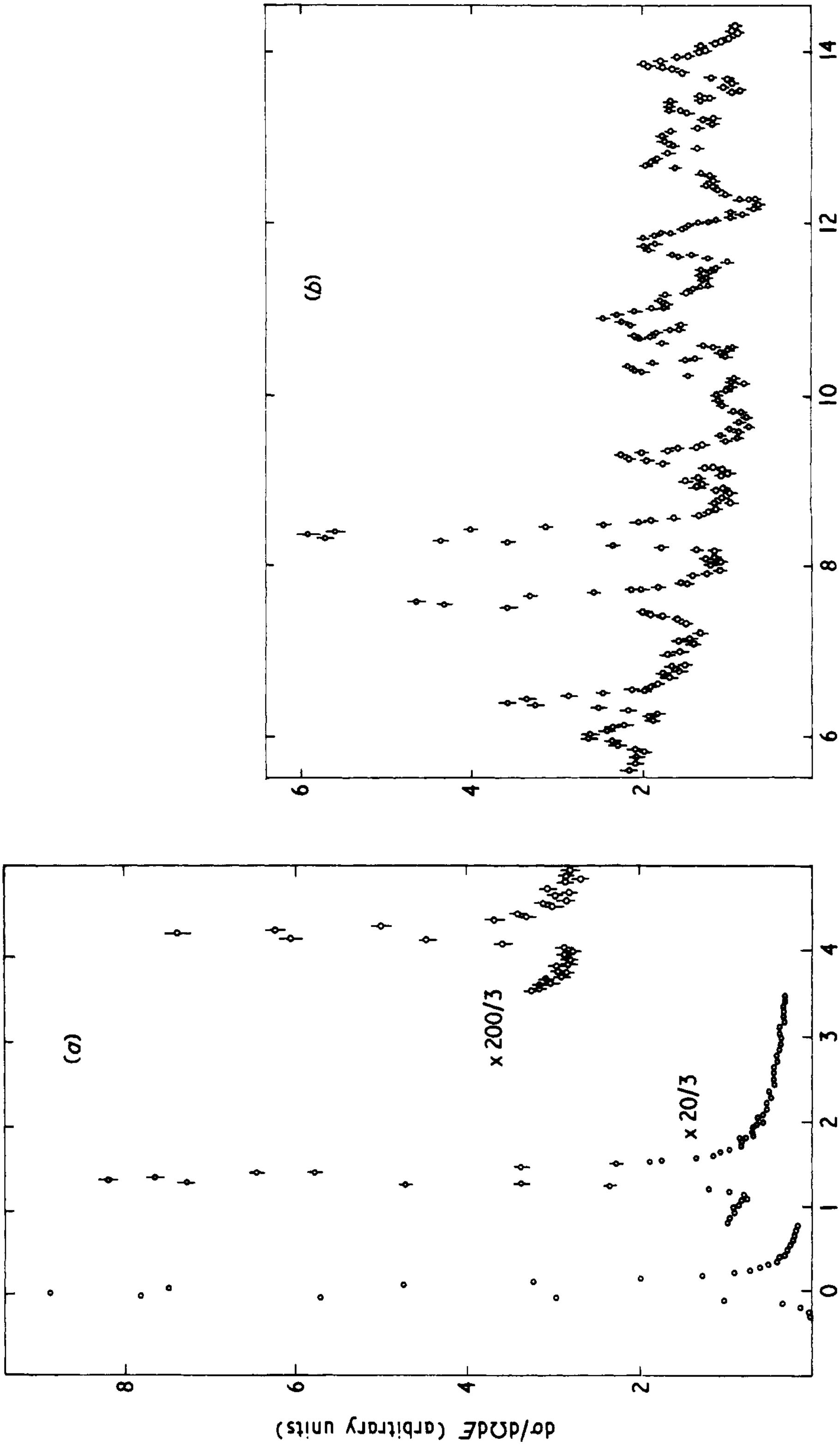

Figure 1. ^{24}Mg excitation energy spectrum. (*a*) $0 < E_x < 5{\cdot}0$ MeV, $E_i = 91{\cdot}5$ MeV, $\theta = 120°$. (*b*) $5{\cdot}0 < E_x < 14{\cdot}0$ MeV, $E_i = 91{\cdot}5$ MeV, $\theta = 120°$.

of the data accumulated on elastic peaks was typically 2%, while for inelastic data the accuracy varied from 1·5% to 5% depending on the count rates and on the ratio of the inelastic levels to the radiation tail. A background measurement was made for each experimental run but it was usually negligibly small.

4. Data analysis

4.1. Determination of inelastic cross sections

The cross section for the excitation of a given nuclear state was obtained by determining the ratio of the inelastic peak area to that of the elastic peak and by calculation of the elastic scattering cross section using the known parameters of the nuclear ground state. The latter cross section was obtained for each energy and angle used in the experiment using the phase shift code of Rawitscher and Fischer (1961) with parameters (Curran *et al* 1972) given by

$$c = 2{\cdot}985\ \mathrm{fm}, \qquad t = 2{\cdot}333\ \mathrm{fm}$$

where c is the half-density radius and t is the skin thickness of the Fermi distribution.

The experimental data were corrected for the effects of detector spacings, efficiencies and percentage energy bite, incident charge and spectrometer field calibration to obtain the differential cross section as a function of excitation energy before proceeding with the lineshape analysis. Calculations of the elastic peak line shape based on the various contributing factors are possible (Bergstrom 1967) if the incident electron spectrum and the detection efficiency function are accurately known but we have simply fitted a phenomenological shape to the elastic peaks, consisting basically of a gaussian and a hyperbola on either side of the peak centre. A best fit was obtained by minimizing χ^2 with respect to variations in the phenomenological parameters using the code VA04A of Powell (1964). An example of such a fit is shown in figure 2. The integration limit for the elastic peak area was usually 1·0 MeV.

The effects which contribute to the shape of a bound inelastic level are the same as those determining the elastic peak shape except that, whereas the incident electron spectrum width and straggling losses are constant on an absolute energy scale, the detector contribution is a constant percentage of the final energy due to the constant dispersion of the magnetic spectrometer. The latter effect is known and the former may be deduced from the elastic peak shape and a width correction factor α_j may be defined for each inelastic peak. Thus, if $f(E)$ is the observed functional shape of the elastic peak, the inelastic spectrum at excitation energy E may be written as

$$F(E) = \sum_{j=1}^{N} h_j f((E-E_j)/\alpha_j) + A/E + B/E^2 + C$$

where E_j and h_j are the excitation energy and height of the jth state and A, B and C are constants. The E^{-1} term represents the contribution to the radiation tail of the elastic peak due to emission of hard photons, the E^{-2} term represents the collision and ionization part of the tail and the constant term arises from background. A typical example of the results of this spectrum fitting procedure is shown in figure 3 where the data between 8·0 and 10·0 MeV excitation energy in ^{24}Mg are presented for $E_i = 70{\cdot}9$ MeV, $\theta = 120°$. The elastic peak radiation tail (plus background), the sum of the elastic peak tail and

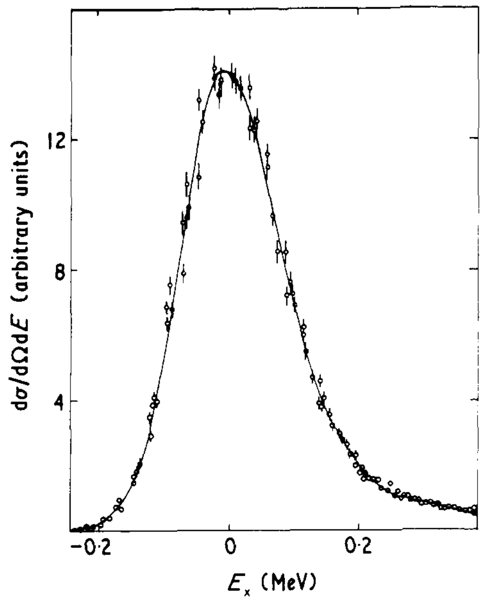

Figure 2. ^{24}Mg elastic scattering peak, $E_i = 73{\cdot}8$ MeV, $\theta = 153°$. The full curve is the best fit using a phenomenological peak shape.

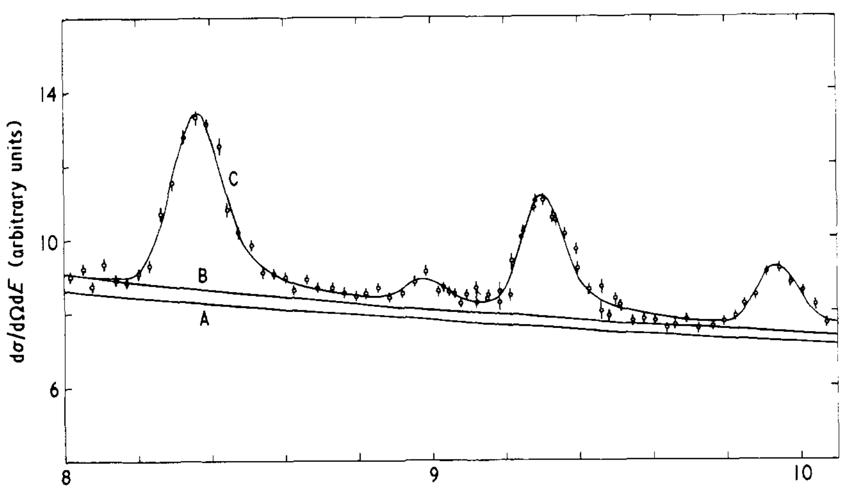

Figure 3. Lineshape analysis of a spectrum. Curve A is the elastic peak radiation tail. Curve B is A plus the radiation tails of lower excited states. Curve C the best fit to the spectrum.

all contributions due to states with excitation energy less than 8·0 MeV, and the final fit to the region are shown with the data.

As a check on the consistency of the above approach the radiation tail was calculated for all spectra using the formalism of Maximon and Isabelle (1964) and was compared to the fitted tail. In all cases the shape was correct to better than 5 % of the height of the inelastic peaks although normalization was required to give absolute agreement. This normalization is attributed to the effects of spectrometer rescattering.

The result of this lineshape fitting procedure is the determination of the excitation energies of the inelastic levels and the ratios of the inelastic peak areas to that of the elastic peak. The results for the excitation energies of the 19 levels of ^{24}Mg observed in this experiment are presented in table 2 together with the errors and spin–parity assignments. The latter are discussed in § 5 and the former in § 4.3. The results for the area ratios, A_{IN}/A_{EL}, are presented in table 3.

Many other excitations were observed in this experiment but are not being presented here either because they were strongly excited in too few spectra or because the errors are large.

Table 2. The observed states of ^{24}Mg.

E_x (MeV)	Error (MeV)	J^π
1·358	0·011	2^+
4·228	0·012	2^+
6·003	0·017	4^+
6·420	0·015	0^+
7·586	0·018	3^-
8·366	0·019	3^-
9·296	0·020	$(2^+, 0^+)$
9·968	0·022	1^+
10·352†	0·024	$2^+, 4^+$
10·695	0·026	1^+
11·1‡		$3^-, (2^+)$
11·382	0·040	2^+
11·855	0·032	$(1^-, 3^-)$
11·990	0·025	3^-
12·388	0·032	3^-
12·522	0·030	2^+
12·706	0·029	2^-
12·990	0·029	2^+
13·371	0·027	2^-

† Doublet.
‡ Triplet.

4.2. *Phase shift analysis*

The most serious restriction on the applicability of the results derived in PWBA arises from the assumption that the electron waves are plane waves. The incoming and outgoing electron waves are distorted in the static Coulomb field of the nucleus and a proper treatment requires the use of electron wavefunctions obtained from a solution of the Dirac equation for an electron in this field (DWBA). When this is done the simplicity of the Born approximation is lost, but it can be retained in the low and intermediate momentum transfer region, and for $Z < 20$, by the calculation of correction factors $f_c(E_i, \theta, L)$ defined by

$$f_c(E_i, \theta, L) = \frac{(d\sigma/d\Omega)_{DWBA}}{(d\sigma/d\Omega)_{PWBA}}$$

which may then be applied to the experimental data to obtain effective PWBA cross sections (Schucan 1968, Drechsel 1968, Chertock *et al* 1970).

Table 3. Area ratios.

Run	1	2	3	4	5	6	7	8	9	10
E_x (MeV)	$\times 10^{-3}$	$\times 10^{-3}$	$\times 10^{-2}$	$\times 10^{-2}$	$\times 10^{-3}$	$\times 10^{-4}$	$\times 10^{-3}$	$\times 10^{-3}$	$\times 10^{-1}$	$\times 10^{-3}$
1·37	147·0	142·0	48·7	47·6	43·4	381·0	—	69·4	21·5	4·40
4·23	9·10	8·72	3·06	2·97	—	20·3	—	3·78	1·24	—
6·00	1·46	2·10	1·65	1·80	—	0·86	—	0·65	2·02	—
6·43	3·17	3·22	7·47	0·79	—	12·7	—	1·86	—	—
7·59	6·77	6·94	3·54	3·96	—	7·87	—	2·55	—	—
8·37	9·57	12·1	5·28	6·19	—	11·5	—	3·63	—	—
9·30	2·69	3·03	0·79	0·85	0·89	8·26	1·70	1·37	—	—
9·97	1·09	4·81	0·40	1·28	2·54	4·38	3·19	0·28	—	—
10·35	2·79	2·86	1·20	1·43	0·70	6·96	1·53	1·10	—	—
10·70	2·60	10·5	0·83	2·13	5·54	11·9	6·71	—	—	—
11·1	6·11	15·2	2·88	6·70	—	10·9	5·76	—	—	—
11·38	0·98	—	0·36	0·72	—	3·03	—	—	—	—
11·86	1·85	—	0·92	—	—	2·29	—	—	—	—
11·99	1·00	2·80	0·57	1·51	—	1·77	—	—	—	—
12·39	0·99	—	0·55	—	—	1·19	—	—	—	—
12·52	1·13	3·47	0·40	1·47	—	2·92	—	—	0·74	—
12·71	2·43	5·66	0·85	2·32	—	3·96	3·10	—	1·39	—
12·99	2·14	6·98	0·84	2·51	—	4·44	3·43	—	1·17	—
13·37	1·85	9·42	0·81	3·70	1·65	3·86	4·32	—	2·10	—

The inelastic scattering form factors are given by

$$F^2_{\mathrm{IN}}(E_i, \theta, L) = \frac{A_{\mathrm{IN}}}{A_{\mathrm{EL}}} \frac{\sigma_{\mathrm{EL}}(E_i, \theta)}{\sigma_{\mathrm{M}}} R$$

where A_{IN} and A_{EL} are the peak areas (inelastic and elastic) obtained from spectrum fitting, $\sigma_{\mathrm{EL}}(E_i, \theta)$ is the elastic scattering cross section, σ_{M} is the Mott cross section, and R is the ratio of the total radiative corrections for inelastic scattering to that of the elastic scattering. This ratio, R, was calculated using the formalism of Maximon (1969) and the correction was less than 1% in all cases. The form factors thus obtained for the states at 1·37 MeV (2^+), 6·00 MeV (4^+), 7·6 MeV (3^-), 9·97 MeV (1^+) and 13·37 MeV (2^-) were analysed in DWBA using the DUELS code of Tuan *et al* (1968) within the context of the Tassie model and the parameters c_{tr}, t_{tr}, and the reduced transition probability for each level were obtained. In addition, the correction factors $f_c(E_i, \theta, L)$ were obtained for each energy, angle, and multipolarity by repeating the calculations in PWBA and this enabled the calculation of the equivalent Born approximation form factors $F^2_{\mathrm{B}}(q)$, defined by

$$F^2_{\mathrm{B}}(q) = F^2_{\mathrm{IN}}(E_i, \theta, L)/f_c(E_i, \theta, L)$$

for each state excited in the experiment. The 0^+ state at 6·43 MeV was analysed by using correction factors deduced from the elastic scattering analysis. The form factors, F^2_{B}, obtained in this way for each state excited in the present experiment are given in table 4.

All states were then analysed in PWBA and a consistency check was of course obtained for those states for which the complete DWBA analysis had been carried out. Both Tassie and Helm model fits were obtained for the states with $E_x < 10{\cdot}0$ MeV but only the Helm model was used for electric transitions above this energy since the Tassie model contains no possible transverse electric strength other than the small Siegert contribution. In the Tassie model c_{tr}, t_{tr} and $B(XL)$ were varied. The variables in the Helm model were β_L and R, g being fixed at the value obtained for elastic scattering, namely $g = 1{\cdot}01$ fm. Several electric transitions above 10·0 MeV display quite strong transverse cross sections and for these γ^0_L was also considered a free parameter. The form factors for the magnetic states in the Helm model analysis contain two radial parts $j_{L-1}(q\bar{R})$ and $j_{L+1}(q\bar{R})$ with corresponding coefficients γ^-_L and γ^+_L. For this reason the radial parameters were fixed, following Rosen *et al* (1967) at the values $\bar{R} = 1{\cdot}25\ A^{1/3}$ fm and $\bar{g} = 1{\cdot}02$ fm.

The range of momentum transfer available in the present experiment was insufficient to enable the determination of two radial parameters independently to great accuracy. For this reason it is useful to give the results for the transition radius R_{tr} for each state since R_{tr} is determined to greater accuracy than either of the two principal radial parameters. R_{tr} is defined by Rosen *et al* (1967).

The strong correlation between the parameters c_{tr} and t_{tr} is illustrated in figure 4 where the χ^2 contours in the c_{tr}–t_{tr} plane are drawn. The errors in c_{tr} and t_{tr} are proportional to the projection of the major axis of an ellipse onto the respective axes. Also shown is a line of constant R_{tr} and since this line only deviates from the major axis by about 15°, the error in R_{tr} is much smaller than that in either c_{tr} or t_{tr} individually.

4.3. Errors estimation

The errors in the excitation energies of table 2 consist of two contributions, the statistical variation in the fitted position and the possible systematic error due to the inaccuracy of

Table 4. Equivalent PWBA form factors squared (absolute errors given below each F_B^2 value).

E_x (MeV)	Factor	Run 1	2	3	4	5	6	7	8	9	10
1·37	10^{-2}	1·50	1·39	1·51	1·38	0·97	0·97	—	1·18	1·11	0·247
		0·07	0·07	0·08	0·07	0·05	0·05	—	0·06	0·06	0·025
4·23	10^{-4}	9.26	8·55	9·48	8·51	—	5·21	—	6·50	6·26	—
		0·65	0·60	0·47	0·43	—	0·50	—	0·65	0·56	—
6·00	10^{-4}	1·23	1·71	4·24	4·26	—	0·18	—	0·94	8·14	—
		0·18	0·26	0·21	0·21	—	0·09	—	0·08	0·80	—
6·43	10^{-4}	3·30	3·21	2·68	2·61	—	3·12	—	3·16	—	—
		0·17	0·32	0·13	0·21	—	0·16	—	0·16	—	—
7·59	10^{-4}	6·45	6·44	10·1	10·3	—	1·90	—	4·08	—	—
		0·45	0·65	0·5	0·5	—	0·13	—	0·29	—	—
8·37	10^{-4}	9·15	8·16	15·1	16·1	—	2·78	—	5·83	—	—
		0·64	0·80	0·8	0·8	—	0·19	—	0·41	—	—
9·30	10^{-4}	2·84	3·06	2·56	2·56	2·16	2·16	2·66	2·42	—	—
		0·17	0·37	0·18	0·31	0·32	0·15	0·27	0·15	—	—
10·35†	10^{-5}	4·15	—	12·5	—	—	1·32	—	1·43	—	—
		0·80	—	1·3	—	—	1·3	—	0·86	—	—
11·1‡	10^{-4}	4·22	12·2	6·41	15·6	—	1·65	6·92	—	—	—
		0·51	1·5	0·65	1·2	—	0·34	0·83	—	—	—
11·38	10^{-4}	1·00	—	1·11	2·08	—	0·77	—	—	—	—
		0·18	—	0·13	0·23	—	0·15	—	—	—	—
11·86	10^{-4}	1·76	—	2·64	—	—	0·56	—	—	—	—
		0·18	—	0·16	—	—	0·06	—	—	—	—
11·99	10^{-4}	0·96	2·60	1·63	3·94	—	0·43	—	—	—	—
		0·14	0·40	0·17	0·32	—	0·05	—	—	—	—
12·39	10^{-4}	0·95	—	1·57	—	—	0·29	—	—	—	—
		0·11	—	0·16	—	—	0·06	—	—	—	—
12·52	10^{-4}	1·12	3·30	1·23	4·12	—	0·72	—	—	3·46	—
		0·13	0·56	0·18	0·50	—	0·06	—	—	0·35	—
12·99	10^{-4}	2·12	6·65	2·56	7·00	—	1·03	5·06	—	5·52	—
		0·22	0·47	0·18	0·50	—	0·93	0·46	—	0·44	—
9·97§	10^{-5}	—	2·52	—	2·01	3·19	—	2·89	—	—	—
		—	0·25	—	0·30	0·22	—	0·14	—	—	—
10·70§	10^{-5}	—	5·58	—	3·00	6·63	—	5·79	—	—	—
		—	0·33	—	0·21	0·33	—	0·29	—	—	—
12·7§	10^{-5}	—	1·91	—	2·48	—	—	1·58	—	2·65	—
		—	0·23	—	0·17	—	—	0·16	—	0·15	—
13·37§	10^{-5}	—	4·27	—	5·15	1·65	—	3·17	—	5·06	—
		—	0·26	—	0·31	0·25	—	0·22	—	0·60	—

† The 4^+ component only is given.
‡ The form factors given are those obtained after subtraction of the 10·93 MeV level contribution.
§ The form factors given for magnetic transitions are $F_T^2 = F_B^2/(\frac{1}{2}+\tan^2\frac{1}{2}\theta)$.

the Rawson constant. For the former the standard error in the mean was used and was added to the 0·1% error in the latter.

Errors in the form factors could arise from several sources:

(i) detector efficiencies, 1·5%;

(ii) SEM efficiency, less than 1% since this measurement is relative to the previous measurement for elastic data;

(iii) Elastic peak area, 1·0%–3·0%;

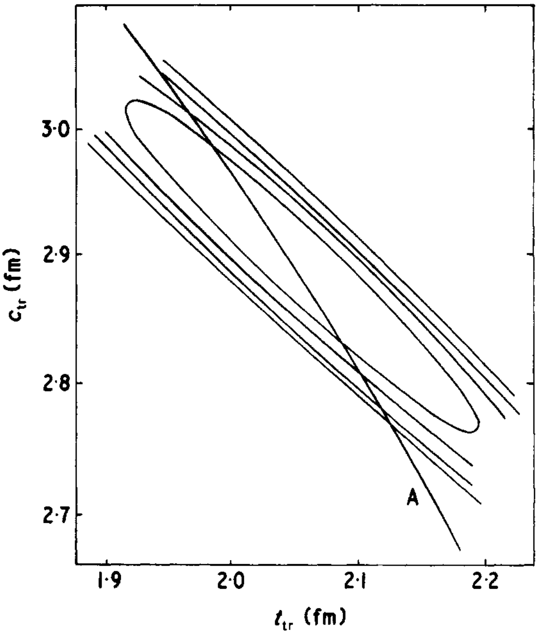

Figure 4. The χ^2 contours on the c_{tr}–t_{tr} plane for the 1·37 MeV (2^+) state. Curve A is the line of constant R_{tr} = 4·10 fm.

(iv) Elastic cross section, 1% at the lowest momentum transfer used and 3·5% at the highest;

(v) Inelastic peak areas, this includes the statistical errors in the raw data and errors due to fitting of overlapping states. The resultant error varied from 1·0% to 50% but was typically of the order of 7%;

(vi) Coulomb correction factors, such an error will be present due to the model dependence of these factors, but Drechsel (1968) has shown this effect to be small.

Thus the principal contributor to the error in the form factors is the error in the determination of the inelastic peak areas.

The errors quoted for the spectroscopic parameters of each state in § 5 are statistical only, but the possible systematic error due to the model dependence of these parameters is discussed by Singhal *et al* (1974). The statistical errors were determined following the procedure outlined by Cline and Lesser (1970).

5. Results

In this section the results obtained for each of the states of ^{24}Mg excited in the present experiment are presented and discussed. We begin by summarizing in tables 5 and 6 the parameters obtained for each transition using the Tassie and Helm models. No errors have been quoted for the parameters c_{tr} and t_{tr} of the Tassie model since they are strongly correlated and the momentum transfer range available in the present experiment was insufficient to allow accurate determination of two radial parameters. A typical error in these quantities is 0·8 fm. The transition radius is, however, well determined and the error is given for each state. In some cases, particularly for the higher

Table 5. Results for the states with $E_x < 11$ MeV.

		Tassie model				Helm model		
E_x (MeV)	J^π	c(fm)	t(fm)	$B(XL\uparrow)e^2$ fm^{2L}	R_{tr}(fm)	R(fm)	$B(XL\uparrow)e^2$ fm^{2L}	R_{tr}(fm)
1·37	2^+	2·88	2·06	420 ± 25	$4·11 \pm 0·08$	3·03	411 ± 23	$4·03 \pm 0·07$
4·23	2^+	2·91	2·08	$26·3 \pm 6·0$	$4·14 \pm 0·30$	3·10	$25·5 \pm 4·0$	$4·09 \pm 0·20$
6·00	4^+	2·48	1·93	$(4·2 \pm 1·0) \times 10^4$	$4·90 \pm 0·70$	3·0	$(3·6 \pm 1·0) \times 10^4$	$4·50 \pm 0·50$
6·43	0^+					5·14	$6·7 \pm 0·4$(ME)	$6·05 \pm 0·20$
7·59	3^-	2·68	2·08	$(1·36 \pm 0·22) \times 10^3$	$4·57 \pm 0·40$	3·17	$(1·30 \pm 0·16) \times 10^3$	$4·39 \pm 0·22$
8·37	3^-	2·61	2·09	$(2·0 \pm 0·2) \times 10^3$	$4·55 \pm 0·38$	3·03	$(1·80 \pm 0·20) \times 10^3$	$4·28 \pm 0·22$
9·30	2^+	3·18	2·36	$12·0 \pm 2·0$	$4·62 \pm 0·30$	3·56	$11·3 \pm 1·5$	$4·45 \pm 0·19$
9·97	1^+	2·45	2·90	$(1·38 \pm 0·20) \times 10^{-2}$	$2·83 \pm 0·30$		$(1·34 \pm 0·15) \times 10^{-2}$	$2·70 \pm 0·20$
10·35	4^+					3·0	$(1·2 \pm 0·4) \times 10^4$	4·5
10·70	1^+	2·64	2·90	$(3·11 \pm 0·40) \times 10^{-2}$	$2·91 \pm 0·40$		$(3·15 \pm 0·30) \times 10^{-2}$	$2·74 \pm 0·30$

Table 6. Results for the states with $E_x > 11$ MeV.

E_x (MeV)	J^π	Helm model R(fm)	γ^0	$B(XL\uparrow)e^2\text{fm}^{2L}$	R_{tr}(fm)
11·1	3^-	3·03†	2·0	$6{\cdot}2\times10^2$	4·3
11·38	2^+	3·10†	$0{\cdot}4\pm0{\cdot}2$	$2{\cdot}5\pm0{\cdot}7$	4·1
11·86	$(1^-, 3^-)$	3·03†	—	$2{\cdot}6\times10^{-6}$(E1) $(3{\cdot}4\pm0{\cdot}5)\times10^2$(E3)	4·3
11·99	3^-	3·03†	$1{\cdot}0\pm0{\cdot}2$	$(1{\cdot}4\pm0{\cdot}2)\times10^2$	4·3
12·39	3^-	3·03†	—	$(2{\cdot}0\pm0{\cdot}2)\times10^2$	4·3
12·52	2^+	3·10†	$0{\cdot}63\pm0{\cdot}05$	$2{\cdot}2\pm0{\cdot}4$	4·1
12·7‡	2^-	$0{\cdot}42\pm0{\cdot}08$	$1{\cdot}6\pm0{\cdot}3$	$0{\cdot}26\pm0{\cdot}10$	$2{\cdot}5\pm1{\cdot}0$
12·99	2^+	3·10†	$0{\cdot}85\pm0{\cdot}05$	$3{\cdot}7\pm0{\cdot}6$	4·1
13·37‡	2^-	$0{\cdot}63\pm0{\cdot}11$	$2{\cdot}2\pm0{\cdot}4$	$0{\cdot}58\pm0{\cdot}20$	$2{\cdot}5\pm1{\cdot}0$

† Parameter fixed at value obtained for a lower energy transition of the same multipolarity.
‡ γ^- and γ^+ are given under R and γ^0 respectively.

excitation electric states where both Coulomb and transverse contributions occur, the radial parameters were fixed at the values obtained for lower energy transitions of the same multipolarity and such cases are indicated in the tables. Certain entries in the tables require further explanation, for example the symbol 'ME', but such entries are explained in the discussion on the particular level concerned.

5.1. The 1·37 MeV state

The level observed with $E_x = 1{\cdot}358\pm0{\cdot}011$ MeV is the $J^\pi = 2^+$ member of the ground state rotational band and it shows the typical enhancement of collective transitions by inelastic electron scattering. The form factors F_B^2 are shown in figure 5 together with the best fit obtained using the Tassie model. The Helm model fit shows no observable difference over the range of momentum transfer shown. The resulting spectroscopic parameters are shown in table 5.

The determination of the reduced transition probability of this level has received much attention in the literature in recent years largely because of the substantial disagreement between the results obtained using different experimental techniques (Endt and Van der Leun 1967, Herman and Kalus 1970). The recent results, however, are shown in table 7 and it can be seen that good agreement is now obtained.

Using the mean of the two model results obtained in the present experiment the collective enhancement of this excitation is $G = 20{\cdot}0\pm1{\cdot}0$. Comparison of the form factors with the predictions of various nuclear models is presented in § 6.

5.2. The 4·23 MeV state

There are two states of ^{24}Mg at this excitation energy, the $J^\pi = 4^+$ member of the ground state rotational band at 4·12 MeV and the $J^\pi = 2^+$ base of the $K = 2$ band at 4·239 MeV. Only one peak was observed in this experiment at $E_x = 4{\cdot}228\pm0{\cdot}013$ MeV, and the momentum transfer dependence of the form factors (figure 5) shows conclusively that the observed state has $J^\pi = 2^+$. This suppression of the $K = 0$, $J^\pi = 4^+$ level has been noted by several authors (eg Crawley and Garvey 1967, Horowitz *et al* 1969). The upper limit for the $K = 0$ state cross section measured by Horowitz *et al* (1969)

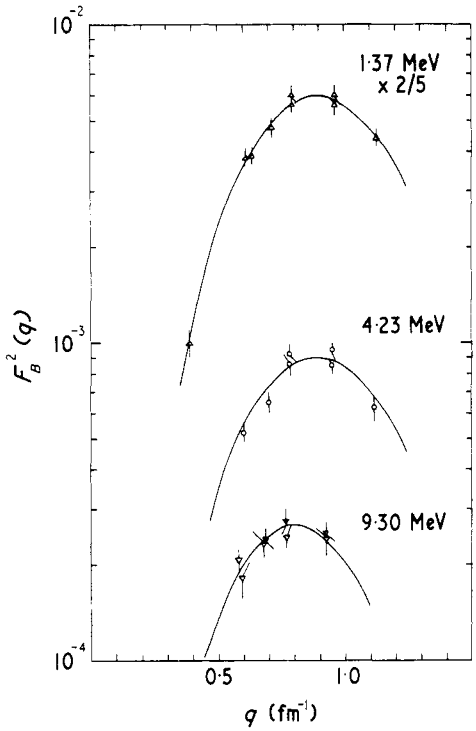

Figure 5. $F_B^2(q)$ for the 2^+ states at 1·37 MeV, 4·23 MeV and 9·30 MeV.

Table 7. The $B(E2\uparrow)$ value of the 1·37 MeV state.

Method	$B(E2\uparrow)e^2\,fm^4$	Reference
Coulomb excitation	416 ± 21	Häusser *et al* (1970)
Coulomb excitation	420 ± 20	Vitoux *et al* (1970)
(γ, γ')	765 ± 90	Herman and Kalus (1970)
(γ, γ')	442 ± 34	Swann (1971)
(e, e′)	455 ± 45	Titze (1969)
(e, e′)	446 ± 45	Nakada and Torizuka (1972)
(e, e′)	420 ± 25	Present work

using inelastic proton scattering was only one eighth that of the $K = 2$, $J^\pi = 4^+$ state at 6·0 MeV.

The form factors obtained for the 4·23 MeV level were therefore analysed in both Tassie and Helm models assuming an E2 transition and the best fit obtained is shown with the data in figure 5, and the results are given in table 5. The $B(E2)$ value obtained in the present experiment is compared with other results in table 8 where it can be seen that good agreement is obtained. The collective enhancement deduced from the present result is $G = 1{\cdot}2 \pm 0{\cdot}2$.

5.3. *The 6·00 MeV state*

The transition from the ground state to the $J^\pi = 4^+$ level at 6·00 MeV has been observed

Table 8. The $B(E2\uparrow)$ value of the 4·23 MeV state.

Method	$B(E2\uparrow)e^2$ fm^4	Reference
Doppler shift attenuation	$23{\cdot}0 \pm 10{\cdot}0$	Robinson and Bent (1968)
Doppler shift attenuation	$21{\cdot}0 \pm 4{\cdot}0$	Anderson and Ritter (1969)
(α, α')	35·0	Naqib and Blair (1968)
(e, e′)	$24{\cdot}0 \pm 4{\cdot}0$	Titze (1969)
(e, e′) PWBA	$22{\cdot}8 \pm 3{\cdot}7$	Nakada and Torizuka (1972)
(e, e′)	$26{\cdot}0 \pm 4{\cdot}0$	Present work

by inelastic alpha scattering (Naqib and Blair 1968) and by inelastic electron scattering (Junk 1970), but the deduced B(E4) values differ markedly; $B(E4\uparrow) = 0{\cdot}7 \times 10^4 e^2$ fm^8 from (α, α') and $(4{\cdot}3 \pm 1{\cdot}3) \times 10^4 e^2$ fm^8 from (e, e'). The present measurement, therefore, should resolve this discrepancy.

The 6·00 MeV state was clearly excited in all spectra and the form factors obtained are shown in figure 6 together with the best fit to the data obtained using the Tassie model. The resulting parameters are shown in table 5 where it can be seen that the Helm model results are significantly lower than the corresponding parameters in the Tassie model, although the discrepancy is covered by the statistical error. This discrepancy appears to be greater for the higher multipolarity transitions.

The value of B(E4) obtained using the Tassie model, namely $B(E4) = (4{\cdot}2 \pm 1{\cdot}0) \times 10^4 e^2$ fm^8, is in excellent agreement with the result of Junk (1970) which was obtained using the same model. The model dependence of the electron scattering results cannot explain the discrepancy between the results of the (α, α') and (e, e′) experiments. Rather, even when the assumption of collectivity is justified, the method used to extract B(EL)

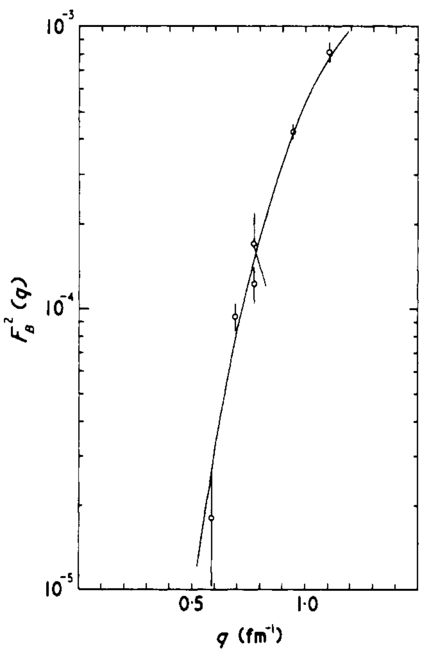

Figure 6. $F_B^2(q)$ for the 4^+ state at 6·00 MeV.

values from the (α, α') data underestimates the contribution of the charge density in the nuclear surface region (Naqib and Blair 1968).

The collective enhancement of this transition is, from the mean of the present two results, $G = 15{\cdot}0 \pm 4{\cdot}0$. Thus the enhancement of the $J^\pi = 4^+$ member of the $K = 2$ band is substantially higher than that of either the $J^\pi = 2^+$ member of the same band or the $J^\pi = 4^+$ member of the ground state band. It will be seen, however, in § 6, that this behaviour is predicted by Hartree–Fock calculations and the classical alpha particle model.

5.4. *The 6·43 MeV state*

The level observed at $E_x = 6{\cdot}420 \pm 0{\cdot}015$ MeV is the first excited 0^+ state of ^{24}Mg. The excitation of monopole transitions by electron scattering is possible since the exciting γ ray is virtual but the treatment of the observed form factors is somewhat different from that presented in § 2 for the general multipolarity L.

The orthogonality of the initial and final states eliminates the first term in the expansion of $j_0(qR)$ giving the result in the Helm model of

$$F_C(q) = \frac{(4\pi)^{1/2}}{Z}\beta_0 \exp(-\tfrac{1}{2}q^2g^2)(j_0(qR)-1). \tag{3}$$

The monopole matrix element is then given by

$$\mathrm{ME} = (4\pi)^{1/2}\beta_0 R^2$$

and the transition radius is found to be given by

$$R_{tr}^2 = R^2 + 10g^2.$$

The present data and those of Titze (1969) are shown in figure 7 together with the best fit to the data obtained using equation (3). The results obtained (using the present

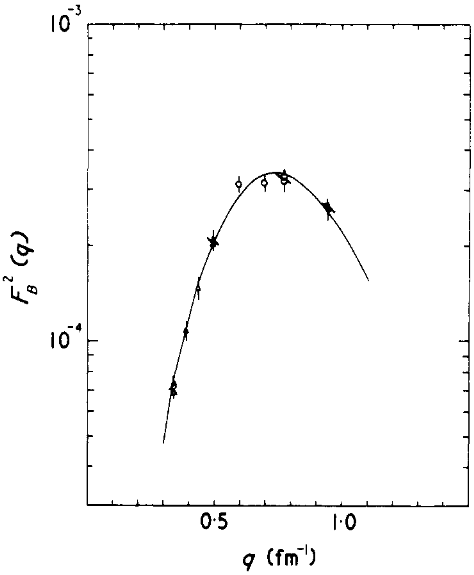

Figure 7. $F_B^2(q)$ for the 0^+ state at 6·43 MeV. The present data, ○, and the data of Titze (1969), △, are shown.

data only) are shown in table 5. The result for the matrix element, ME $= 6{\cdot}66 \pm 0{\cdot}38e\,\mathrm{fm}^2$, is in good agreement with the result of Titze (1969), ME $= 6{\cdot}23 \pm 0{\cdot}62e\,\mathrm{fm}^2$.

Walecka (1962) has shown that the matrix element of monopole transitions is related to the electromagnetic width, $\Gamma_0(\mathrm{e}^+\,\mathrm{e}^-)$, for pair emission to the ground state by

$$\Gamma_0 = \frac{\alpha^2 \hbar c}{135\pi}(E_x)^5 |\mathrm{ME}|^2.$$

The width deduced from our data is $\Gamma_0(\mathrm{e}^+\mathrm{e}^-) = (4{\cdot}0 \pm 0{\cdot}5) \times 10^{-5}$ eV. Unfortunately, no direct measurement of the pair emission measurement has been made.

5.5. The 7·59 MeV state

The form factors for the transition to the state at $E_x = 7{\cdot}586 \pm 0{\cdot}018$ MeV are shown in figure 8 from which it can be seen that the q dependence implies an E3 transition. A state with $J^\pi = 3^-$ is known at $E_x = 7{\cdot}615$ MeV but its energy is just outside the above error limits. The $J^\pi = 1^-$ state at 7·56 MeV could, however, be contributing to the observed strength since, as Eisenberg and Rose (1963) and Torizuka *et al* (1969) have noted, the isospin selection rules imply that $\Delta T = 0$ E1 transitions in self-conjugate nuclei will exhibit a q dependence at low momentum transfer identical to that of E3 transitions. Nevertheless, the energy separation of the two states is 50 keV and if both were contributing to the observed cross section in approximately equal proportions it would have been necessary to fit a doublet state to the data. In no spectrum was this necessary. We have, therefore, assumed that the observed state is the 3^- level at 7·615 MeV.

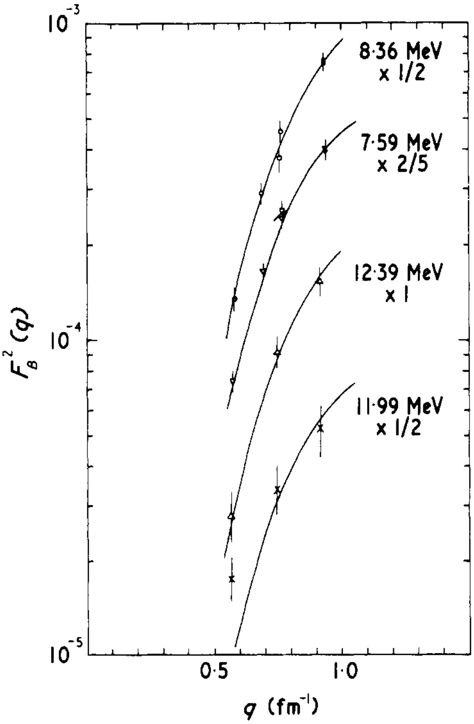

Figure 8. $F_B^2(q)$ for the 3^- states at 7·59 MeV, 8·36 MeV, 11·99 MeV and 12·39 MeV.

The best fit to the data using both Tassie and Helm models is shown in figure 8 with the data, and the resulting parameters are given in table 5. From the deformation parameter obtained by Crawley and Garvey (1967) for this state using inelastic scattering of 17·5 MeV protons one can deduce the collective enhancement of this level. The result is $G = 4{\cdot}9$. (No error is quoted.) This compares favourably with the present result of $G = 5{\cdot}4 \pm 0{\cdot}8$. A comparison with the (α, α') result of Naqib and Blair (1968) is not as good, their result being $G = 3{\cdot}6 \pm 0{\cdot}6$. As has already been pointed out, however, the (α, α') results are consistently lower than the (e, e') values. The previous (e, e') result of Titze (1969) gave $G = 6{\cdot}5 \pm 2{\cdot}2$ but this was obtained using an analysis in PWBA.

5.6. *The 8·36 MeV state*

The level observed at $E_x = 8{\cdot}366 \pm 0{\cdot}019$ MeV has $J^\pi = 3^-$ (Endt and Van der Leun 1967) and has been interpreted by Branford *et al* (1971) as being the second member of a $K^\pi = 0^-$ band based on the $J^\pi = 1^-$ state at 7·56 MeV. The data are shown in figure 8 together with the best fit obtained using the Tassie model. The resulting parameters are shown in table 5.

The enhancement factor deduced from the mean of the Tassie model and Helm model results is $G = 7{\cdot}7 \pm 0{\cdot}8$. The PWBA result of Titze (1969) was $G = 10{\cdot}5 \pm 1{\cdot}7$, but this agrees with the present value when proper corrections have been applied for the effects of Coulomb distortion. Once again the (α, α') result of Naqib and Blair (1968), $G = 4{\cdot}2 \pm 0{\cdot}4$, is lower than the (e, e') results, the ratio being the same as for the 3^- state at 7·6 MeV. The (p, p') result of Crawley and Garvey (1967), however, is $G = 2{\cdot}6$. Thus this excitation is weaker in the (p, p') experiment than the state at 7·6 MeV, in contrast with the (α, α') and (e, e') results.

5.7. *The 9·30 MeV state*

The form factors for the excitation of the state at $E_x = 9{\cdot}296 \pm 0{\cdot}020$ MeV are shown in figure 5, from which it can be seen that $J^\pi = 0^+$ or 2^+. It is possible in principle to distinguish between these two assignments by observing the angular distribution since a small transverse strength must be present if the 2^+ assignment is correct. It was not possible, however, to be conclusive on this point with the present data. The results presented in table 5 were obtained assuming $J^\pi = 2^+$. If the $J^\pi = 0^+$ assumption is made the resulting matrix element is ME $= 6{\cdot}2 \pm 1{\cdot}5e\ \mathrm{fm}^2$. Titze (1969) also observed this state but again could not distinguish between the 0^+ and 2^+ assignments. The resulting $B(\mathrm{E2})$ value was $(11{\cdot}22 \pm 0{\cdot}91)e^2\ \mathrm{fm}^4$, in good agreement with the present results.

In a recent study of the $^{12}\mathrm{C}(^{16}\mathrm{O}, \alpha\gamma)^{24}\mathrm{Mg}$ reaction Wright (1972, private communication) observed three states at this excitation energy and measured the lifetimes by Doppler shift attenuation techniques. The results and deduced γ ray widths, Γ_γ, were:

(*a*) $E_x = 9{\cdot}282$ MeV, $\Gamma_\gamma \simeq 0{\cdot}066$ eV;
(*b*) $E_x = 9{\cdot}300$ MeV, $\Gamma_\gamma \simeq 0{\cdot}0033$ eV;
(*c*) $E_x = 9{\cdot}301$ MeV, $\Gamma_\gamma > 0{\cdot}066$ eV.

The present data yield a ground state width of $\Gamma_0 = 0{\cdot}12 \pm 0{\cdot}02$ eV when the 2^+ assignment is assumed and when the 0^+ assignment is considered the resulting width is $\Gamma_0(e^+, e^-) = 2{\cdot}3 \times 10^{-4}$ eV. The 2^+ assignment is, therefore, only compatible with state (*c*). No ground state transition was, however, observed for this level, while such a transition should have been easily seen if the 2^+ assignment is correct and the strength is as measured in the present experiment. The 0^+ assignment is compatible with each of these widths. Wright, however, observed a strong decay from the 9·301 MeV state to the 2^+ state at 7·35 MeV and concluded that if an E2 transition was responsible the collective enhancement was very high, and this makes the 0^+ assignment unlikely for this state. The decay of the 9·300 MeV level was consistent with $J^\pi = 4^-$, so that once again the 0^+ assignment is not possible. The fast decay of the 3^- state at 13·087 MeV to the 9·282 MeV level (Mayer *et al* 1972) rules out the 0^+ assignment to this level. It would, therefore, appear that 4 states exist at 9·3 MeV in ^{24}Mg.

5.8. The 9·97 MeV state

The state at 9·97 MeV in ^{24}Mg is the $T_Z = 0$ analogue of the $J^\pi = 1^+$ levels of ^{24}Na and ^{24}Al at $E_x \simeq 0{\cdot}46$ MeV. It is, therefore, easily excited by inelastic electron scattering and has been observed by Titze (1969) and Fagg *et al* (1970).

The transverse nature of this transition is seen in figure 9(*a*) where the data obtained at fixed values of momentum transfer are plotted as a function of $\tan^2 \frac{1}{2}\theta$. The data at $q = 0{\cdot}97\ \mathrm{fm}^{-1}$, however, display a significant longitudinal component which suggests the excitation of a second state at this energy and such an excitation could lead to an overestimate of the transverse form factor for the 1^+ state. The $J^\pi = 2^+$, $T = 1$ state at 10·08 MeV (Lawergren *et al* 1968) could, for example, produce such an effect. For this reason the high q point was omitted from the fit but is shown in figure 10 with the other data.

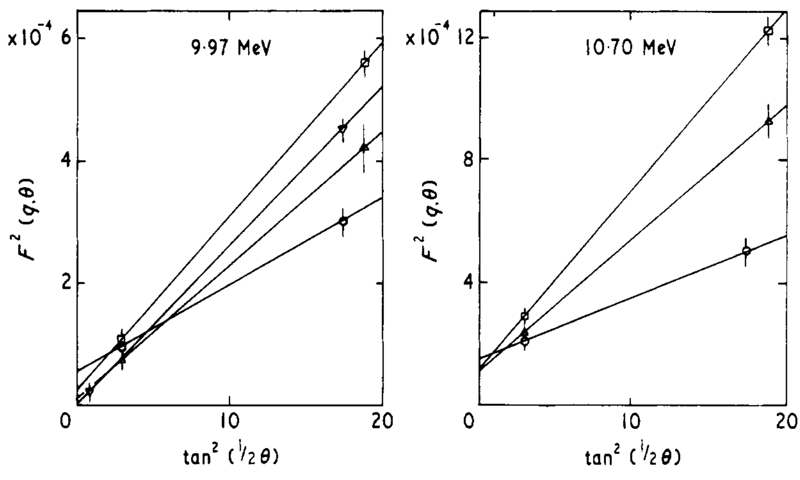

Figure 9. Separation of the longitudinal and transverse components for the 1^+ states at 9·97 MeV and 10·70 MeV at $q = 0{\cdot}97\ \mathrm{fm}^{-1}$(○), $0{\cdot}80\ \mathrm{fm}^{-1}$(△), $0{\cdot}72\ \mathrm{fm}^{-1}$(▽) and $0{\cdot}63\ \mathrm{fm}^{-1}$(□).

The data of Titze (1969) have also been included in the present analysis since at the time of the previous analysis the M1 correction factors were not available. The procedure followed at that time was that the inelastic form factors were calculated using equivalent Born approximation elastic scattering form factors and subsequent application of E2 correction factors. Such a procedure leads to an overestimate of the transition probability. In the present analysis the form factors were calculated using elastic form

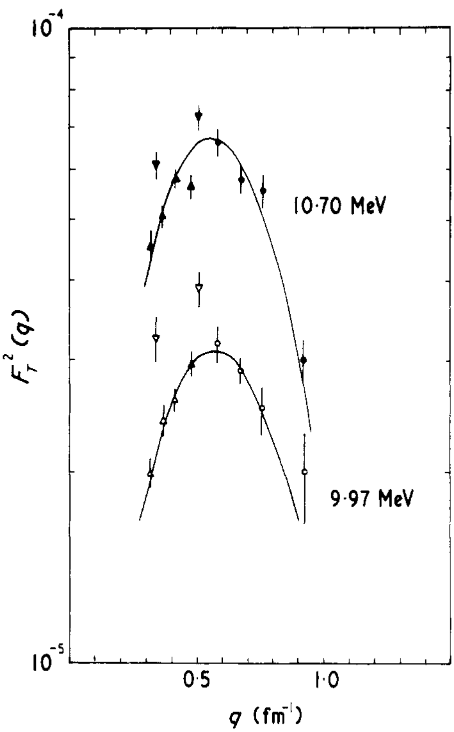

Figure 10. $F_T^2(q) = F_B^2(q)/(\frac{1}{2}+\tan^2\frac{1}{2}\theta)$ for the 1^+ states at 9·97 MeV and 10·70 MeV. The curves are the best fits obtained using the data of Titze (1969), △ and ▲, and of the present experiment, ○ and ●. Also shown are the data of Fagg *et al* (1970), ▽ and ▼.

factors calculated using the Rawitscher–Fischer phase shift code and the Fermi distribution with the parameters given in § 4.1. In addition the form factors for the two $J^\pi = 1^+$ states observed by Titze (1969) at 9·85 MeV and 9·97 MeV were added since the present experiment is sensitive to the unresolved sum.

The data were analysed within the context of the Tassie model using the DUELS phase shift code and the best fit parameters obtained are given in table 5. In addition the correction factors, as defined in § 4.1, were calculated to obtain the equivalent Born approximation form factors and these were used to obtain the best fit to the data using the Helm model. The results are again shown in table 5 and the best fit is shown in figure 10. The agreement obtained both for the transition probabilities and the transition radii in the two models is very good and is a little surprising since the models differ markedly in their assumptions with respect to magnetic transitions. The Tassie model includes only a current contribution whereas in the Helm model this contribution is zero and the strength originates solely in the magnetization density. This result, therefore, gives one confidence in the model independence of the parameters quoted.

Two previous measurements of the ground state width of this state exist (excluding the measurement of Titze (1969) which is incorporated in the present analysis). Fagg *et al* (1970) obtained $\Gamma_0 = 7{\cdot}6^{+1{\cdot}6}_{-1{\cdot}4}$ eV by inelastic electron scattering at 180°. The two data points from this experiment are shown with the present results in figure 10. Kuehne *et al* (1967) measured the width by resonant fluorescence scattering, yielding $\Gamma_0 = 5{\cdot}6$ eV.

The discrepancies between these results and the present value of $\Gamma_0 = 4{\cdot}6 \pm 0{\cdot}4$ eV are discussed in § 5.10 in the discussion on the $J^\pi = 1^+$ state at 10·7 MeV.

5.9. The doublet at 10·35 MeV

The state observed at $10{\cdot}352 \pm 0{\cdot}024$ MeV has been assigned $J^\pi = 2^+$ (Endt and Van der Leun 1967). The data obtained in the present experiment, however, were not consistent with the excitation of a singlet $L = 2$ multipolarity but imply the existence of a doublet consisting of the known state and an additional level with higher spin. No significant transverse strength was observed thus limiting the spin assignment to 3^- or 4^+ since any higher multipolarity would require a transition strength of more than 50 Wu.

The procedure adopted in the analysis was as follows. The low momentum transfer data of Titze (1969), which should be insensitive to the higher multipolarity component, were re-analysed using the Helm model and the E2 correction factors of Toepffer and Drechsel (1968), and the best fit obtained was extrapolated to $q = 1{\cdot}0\ \mathrm{fm}^{-1}$. This extrapolation is shown in figure 11 where the discrepancy with the present data is obvious. The extrapolated E2 form factors were subtracted from the present data using the E2 correction factors obtained using DUELS and the form factors thus obtained were analysed using the Helm model by considering both E3 and E4 transitions and application of the appropriate Coulomb corrections. Only the E4 assignment was found to be acceptable

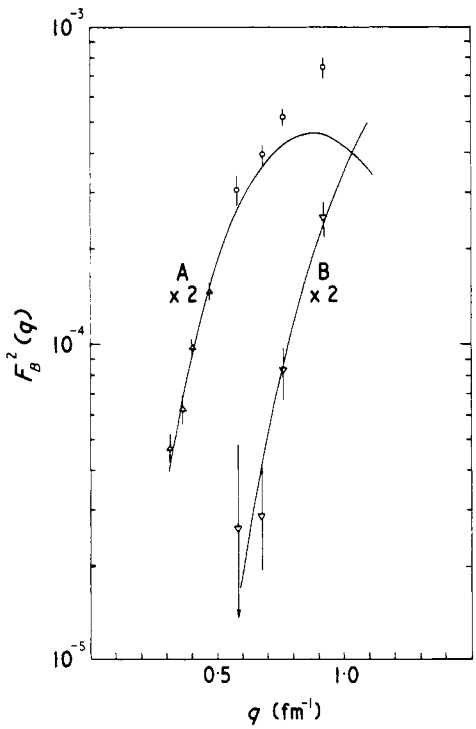

Figure 11. $F_B^2(q)$ for the 10·35 MeV doublet; present experiment ○, and Titze (1969) △. Curve A is the fit to △ and its extrapolation. Curve B is the fit to the residual form factors ▽ as an E4 transition.

and the results are shown in figure 11. The transition probability obtained was

$$B(\mathrm{E4}) = (1{\cdot}2 \pm 0{\cdot}4) \times 10^4 e^2\,\mathrm{fm}^8$$

and the collective enhancement of this transition is $G = 4{\cdot}4 \pm 1{\cdot}5$.

Some evidence for the existence of a doublet at this excitation energy exists from two experimental studies of the ^{23}Na(d, n)^{24}Mg reaction. Fuchs *et al* (1968) observed an $l_p = 2$ stripping pattern for the second component which is compatible with $J^\pi = (3,4)^+$ (assuming $J > 2$). Tang *et al* (1969), however, report an $l_p = 1$ stripping pattern which only allows $J^\pi = 3^-$. The present result, therefore, supports the former experiment. Once source of error in the present analysis is, of course, the necessity for subtraction of the E2 contribution. An electron scattering experiment at higher values of momentum transfer, where the higher multipolarity transition would completely dominate, should provide conclusive evidence on this point.

5.10. The 10·70 MeV state

The separation of the longitudinal and transverse contributions to the form factors obtained at fixed values of momentum transfer, shown in figure 9(*b*), for the transition at $E_x = 10{\cdot}695 \pm 0{\cdot}026$ MeV indicates a strong transverse strength with M1 q dependence and a weak Coulomb strength with (C2, C0) q dependence. Thus the levels at 10·72 MeV ($J^\pi = 1^+$) and 10·68 MeV ($J^\pi = 0^+$) can be identified as the contributing states. Only the magnetic state has been analysed since it dominates at all but the highest value of momentum transfer.

As for the 1^+ state at 9·97 MeV, the data of Titze (1969) were included in the analysis. The values of the parameters of the Tassie model, obtained by phase shift analysis, are given in table 5, together with the Helm model results obtained by application of the correction factors and PWBA analysis. Once again the agreement obtained for the results in the two models is very good. The data and the best fit obtained are shown in figure 10.

The ground state width deduced from the above results for the $J^\pi = 1^+$ state is $\Gamma_0 = (13{\cdot}4 \pm 1{\cdot}2)$ eV. In contrast, the previous (e, e′) measurement of Fagg *et al* (1970) was $\Gamma_0 = (17{\cdot}6^{+3\cdot5}_{-3\cdot0})$ eV, while the (γ, γ') result of Kuehne *et al* (1967) was $\Gamma_0 = 17{\cdot}0$ eV. Similar discrepancies were noted in § 5·8 for the M1 transition at 9·97 MeV. The γ ray energy resolution in the resonant scattering experiment was, however, not sufficient to distinguish between the ground state and first excited state transitions. Kuehne *et al* (1967) estimated the inelastic contribution from calculations of the lineshape in the NaI detector, their results being 10 % for the 10·7 MeV transition and 25 % for the 9·97 MeV transition. More recent measurements of the branching ratios of these states (Lawergren *et al* 1970), however, show that 48 % of the decay of the 10·7 MeV level is due to the 10·7 MeV → 1·37 MeV transition and only 40 % goes to the ground state. Thus the above value of Γ_0 from the (γ, γ') experiment is incorrect and it would be necessary to recalculate the self-absorption corrections before a revised value of Γ_0 could be quoted for the 10·7 MeV state. The result of Lawergren *et al* (1970) for the branching ratio of the 9·97 MeV level is, however, in fair agreement with that used by Kuehne *et al* (1967), namely 30 % decay to the 1·37 MeV level, and this is reflected in the better agreement obtained between the present measurement of Γ_0 and the (γ, γ') result for the 9·97 MeV state.

The discrepancy between the present results and those of Fagg *et al* (1970) for both M1 transitions is not easily explained. One possible source of error may lie in the fact that both the Darmstadt (Titze 1969) and Glasgow measurements were performed relative to the elastic scattering cross section, while the 180° scattering measurement of Fagg *et al* (1970) was an absolute measurement. One possible check on the present results would be provided by a (γ, γ') measurement using a Ge(Li) detector.

5.11. The triplet at 11·0 MeV

The inelastic scattering spectrum fitting program consistently required the presence of three levels between 10·8 and 11·3 MeV, the mean positions being 10·93 MeV, 11·02 MeV and 11·19 MeV. The complexity is such, however, that only the sum of the three contributions could be reliably extracted from the data. The 10·93 MeV state is undoubtedly the 2^+ level observed by Titze (1969). The contribution from this excitation was, therefore subtracted in a manner similar to that described for the 10·35 MeV state, the remaining strength being analysed as a single transition.

The resulting form factors imply that the transition is E3 but with a small E2 admixture. Considerable transverse strength is present. The data were analysed using the Helm model by including β_3 and γ_3^0 as parameters, R being fixed at the value obtained for the 3^- state at 8·36 MeV. The results are given in table 6, and these values may be considered as upper limits on the matrix elements for the E3 transition.

5.12. The 11·38 MeV state

An excitation was observed at $11{\cdot}38 \pm 0{\cdot}04$ MeV in four spectra and the data seem consistent with an E2 transition with a small transverse contribution. The analysis using the Helm model gave $B(\mathrm{E2}) = 2{\cdot}5 \pm 0{\cdot}7 e^2\,\mathrm{fm}^4$ and $\gamma_2^0 = 0{\cdot}4 \pm 0{\cdot}2$.

5.13. The states at 11·86, 11·99 and 12·39 MeV

The excitations observed at 11·86, 11·99 and 12·39 MeV all display a q dependence characteristic of E3 transitions.

The state excited at $E_x = 11{\cdot}855 \pm 0{\cdot}032$ MeV may be the $J^\pi = 1^-$ state given by Endt and Van der Leun (1967) and Highland and Thwaites (1968). This level has isospin $T = 0$ and, therefore, the ground state transition is first order forbidden. The consequences of this for electro-excitation have been observed by Torizuka *et al* (1969) and result in a behaviour at low values of momentum transfer similar to that obtained for E3 transitions. Extrapolation to the photon point gives a value of the reduced transition probability of $B(\mathrm{E1}) = (2{\cdot}6 \pm 1{\cdot}0) \times 10^{-6} e^2\,\mathrm{fm}^2$, but it should be emphasized that observation of such a transition at the photon point would probably arise predominantly via isospin impurities and would, therefore, yield a transition probability greater than the above value. The data were also analysed assuming the state to have $J^\pi = 3^-$, the result being $B(\mathrm{E3}) = (3{\cdot}4 \pm 0{\cdot}5) \times 10^2 e^2\,\mathrm{fm}^6$.

The level observed at $E_x = 11{\cdot}990 \pm 0{\cdot}025$ MeV has a q dependence and angular dependence which indicate an E3 transition with a substantial transverse strength. The Helm model was used to obtain the results shown in table 6. The state being excited is probably the $J^\pi = 3^-$ state at 12·02 MeV given by Endt and Van der Leun (1967) and Highland and Thwaites (1968).

The form factors for the level at $E_x = 12{\cdot}388 \pm 0{\cdot}032$ MeV clearly indicate an E3 transition although no $J^\pi = 3^-$ state has been observed at this energy. No significant transverse strength was observed and the transition probability obtained was $B(\mathrm{E3}) = (2{\cdot}0 \pm 0{\cdot}2) \times 10^2 e^2\ \mathrm{fm}^6$.

The data for the two longitudinal transitions at 11·86 and 12·39 MeV are shown with the E3 transitions at 7·6 and 8·36 MeV in figure 8.

5.14. *The 12·52 MeV state*

The excited state at $E_x = 12{\cdot}522 \pm 0{\cdot}030$ MeV in ^{24}Mg observed in this experiment is quite clearly a $J^\pi = 2^+$ state with a large transverse contribution to the cross section. The dominant transverse form factors are plotted as a function of q in figure 12 together with the best fit to the data obtained using the Helm model. The resulting parameters are shown in table 6.

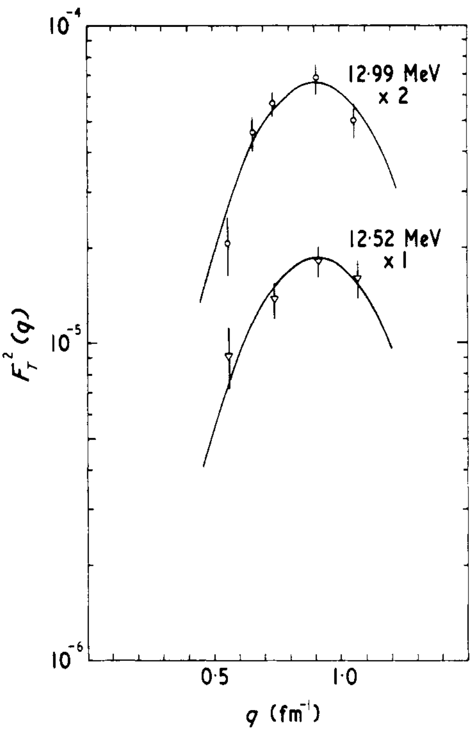

Figure 12. The transverse form factors $F_T^2(q)$ for the 2^+ states at 12·52 MeV and 12·99 MeV.

Goldberg *et al* (1954) observed a 2^+ state at 12·50 MeV using the ^{20}Ne(α, γ)^{24}Mg reaction. Highland and Thwaites (1968) restricted the spin and parity of a level at 12·513 to $(2, 4)^+$ with the 4^+ assignment, however, being the more likely candidate.

5.15. *The 12·71 MeV state*

The q dependence of the observed transition to the state at $12{\cdot}706 \pm 0{\cdot}029$ MeV is, once again, not characteristic of a single multipolarity since the large cross section at the highest momentum transfer appears to rule out a simple E2 transition. In addition, substantial transverse strength is present, and the most probable interpretation of the data is that the two states have $J^\pi = 2^+$ and $J^\pi = 2^-$. Lawergren *et al* (1968) have identified a state in ^{24}Mg with $J^\pi = 2^-$ and $T = 1$ at 12·67 MeV and one would expect the excitation of such a level by inelastic electron scattering. Highland and Thwaites (1968) observed a 2^+ state at 12·74 MeV so that the above interpretation seems plausible.

The procedure adopted, therefore, in the data analysis was to determine the Coulomb strength from the longitudinal–transverse separations at 0·76 and 0·92 fm^{-1} and to assume that the E2 transition had the same radial parameters as the lower excitation 2^+ states. This then enabled the subtraction of the Coulomb contribution from each run. The transverse strength thus obtained was then assumed to be due entirely to the excitation of the 2^- state. This may be an overestimate since there is no way of knowing, *a priori*, what the transverse E2 strength of the competing state will be. The transverse form factors obtained in this way, and corrected for the effects of Coulomb distortion, are shown in figure 13 together with the best fit obtained using the Helm model. The resulting parameters are given in table 6 and the corresponding ground state width is $\Gamma_0 = (1{\cdot}4 \pm 0{\cdot}50) \times 10^{-2}$ eV.

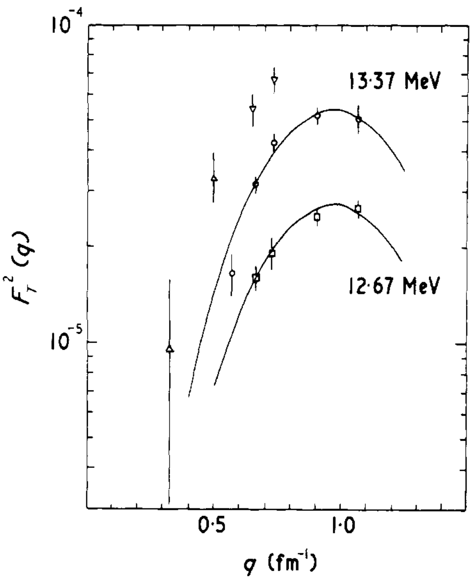

Figure 13. $F_T^2(q) = F_B^2(q)/(\frac{1}{2} + \tan^2 \frac{1}{2}\theta)$ for the 2^- states at 12·67 MeV and 13·37 MeV. Also shown are the data, △, of Fagg *et al* (1970) for the 13·37 MeV state and the integrated $F_T^2(q)$, ▽, from the present experiment.

Mayer *et al* (1972) populated the $J^\pi = 2^-$ state using the ^{23}Na(p, γ)^{24}Mg reaction, measured the absolute strength and observed the branching ratios for γ decay. The results were:

$$(2J+1)\Gamma_\gamma \Gamma_p/\Gamma = 12 \text{ eV}$$

and

$$\Gamma_0/\Gamma_\gamma = 4 \times 10^{-3}.$$

If $\Gamma_p \simeq \Gamma$, which should be a reasonable assumption since $T = 1$, the resulting ground state width is $\Gamma_0 = (1{\cdot}0 \pm 0{\cdot}5) \times 10^{-2}$ eV, in good agreement with the present result.

The 2^+ state at 12·74 MeV has been observed in the ^{23}Na(p, $\alpha\gamma$)^{20}Ne reaction (Stark *et al* 1970) and it, therefore, has a large α width. Thus the isospin is $T = 0$ and it is likely that the transverse strength in electro-excitation will be small, which was the assumption made in the above analysis. The strength of the E2 transition which was subtracted was $B(\text{E2}) = 4{\cdot}0e^2\ \text{fm}^4$.

5.15. The 12·99 MeV state

The form factors for the excitation at 12·990 ± 0·029 MeV are consistent with an E2 transition with a large transverse contribution to the cross section. The data were analysed in the Helm model and the results are given in table 6, the best fit to the dominant transverse form factors being shown in figure 12. The ground state width obtained from these results is $\Gamma_0 = 0{\cdot}22 \pm 0{\cdot}04$ eV.

The transverse contribution to this excitation was observed by Fagg *et al* (1970) by (e, e′) at 180° and the interpretation placed on the data was that it arose from a $J^\pi = 2^-$, $T = 1$ state. The results of Stark *et al* (1970) were quoted in support of this assignment since the latter experiment observed two states with $J^\pi = 2^-$ at $E_x = 12{\cdot}85$ and 12·97 MeV, and it was suggested that the (e, e′) experiment was sensitive to the unresolved sum. This argument is, however, fallacious since the measurements of Stark *et al* (1970) employed the ^{23}Na(p, $\alpha\gamma$)^{20}Ne reaction and the observed states must have $T = 0$. This does not invalidate the 2^- assignment to the electron scattering data but it is unlikely that a $T = 0$ magnetic state would have such a large strength.

In § 6, consideration is given to the possible assignment of $T = 1$ to the 2^+ states observed in this experiment at 12·52 and 12·99 MeV.

5.16. The 13·37 MeV state

The excitation of a state at 13·37 ± 0·05 MeV by electron scattering at 180° has been reported by Fagg *et al* (1970), and the assignment made was $J^\pi = 2^-$, $T = 1$. The present experiment agrees with this assignment for the level at 13·371 ± 0·027 MeV. The transverse nature of the transition can be seen from the longitudinal–transverse separation of the contributing cross sections shown in figure 14 for fixed values of the momentum transfer. The data were analysed using DUELS and the correction factors obtained have been applied to the data before plotting in the figure. The results then obtained using the Helm model are given in table 6 and the ground state width obtained is

$$\Gamma_0 = (4{\cdot}0 \pm 1{\cdot}4) \times 10^{-2}\ \text{eV}.$$

The ground state width obtained in the present experiment is somewhat lower than the result of Fagg *et al* (1970) who obtained $\Gamma_0 = 0{\cdot}13^{+0{\cdot}18}_{-0{\cdot}08}$ eV but this is probably due to the better resolution of the present experiment. In the present study levels were also excited at 13·2 and 13·5 MeV in addition to the main peak at 13·37 MeV but the data did not justify independent analysis. Nevertheless, the integrated transverse strength of this region has been evaluated for the values of momemtum transfer close to those used by Fagg *et al* (1970). The results are compared to those of the previous experiment in figure 13. The agreement is quite good.

Mayer *et al* (1972) observed a resonance in the ^{23}Na(p, γ)^{24}Mg reaction at 13·365 MeV but could not identify the spin and parity. The results of their measurements of the

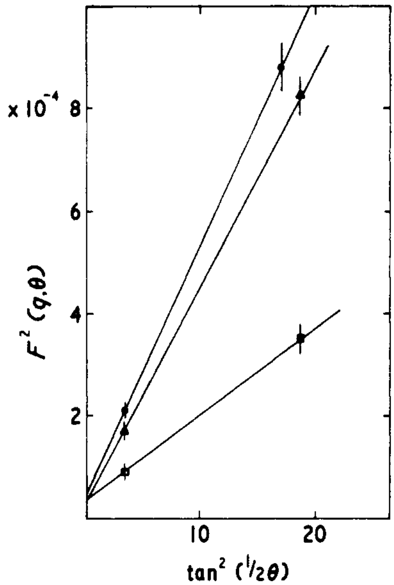

Figure 14. Separation of the longitudinal and transverse components for the 2^- state at 13·37 MeV at q = 0·97 fm^{-1}(○), 0·80 fm^{-1}(△) and 0·63 fm^{-1}(□).

absolute strength and ground state branching ratio were:

$$(2J+1)\Gamma_p\Gamma_\gamma/\Gamma = 2\,\text{eV}$$

$$\Gamma_0/\Gamma_\gamma = 0{\cdot}06.$$

Hence if $J^\pi = 2^-$ and $T = 1$, the α width may be neglected, and one obtains

$$\Gamma_0 = (2{\cdot}4 \pm 1{\cdot}2) \times 10^{-2}\,\text{eV},$$

which is in good agreement with our result. One further piece of evidence for the $T = 1$ assignment is that no such resonance was observed in the ^{20}Ne(α, γ)^{24}Mg reaction study by Highland and Thwaites (1968).

6. Discussion

The form factors obtained in an electron scattering experiment can provide a sensitive test of nuclear models. In this section, therefore, the results of the present experiment are compared with the predictions of the classical alpha particle model, the Nilsson model, and Hartree–Fock calculations for ^{24}Mg. In addition, the $T = 1$ states of ^{24}Mg excited in the present experiment are discussed within the framework of the independent particle shell model.

6.1. The classical alpha particle model

The classical alpha particle (CAP) model has been applied to the 4N nuclei in the s–d shell by Hauge *et al* (1971). The model assumes that the internal α particles are harmonically bound in a semi-rigid molecular structure and the observed properties are then predicted by methods analogous to those used in molecular mechanics and are found to depend primarily on the symmetry of the assumed structure.

Hauge *et al* (1971) considered all possible configurations of α particles for ^{24}Mg and concluded that only the bitetrahedron shape with symmetry D_{2h} produced an energy spectrum in agreement with experiment. The electron scattering form factors for the states in rotational bands based on the ground state vibration were calculated and we compare our results with these predictions. The radial parameters of the model were determined from elastic electron scattering leaving only one parameter, the angle θ defined in the above reference, to be determined by the inelastic scattering results.

The parameter θ was varied to obtain an optimum fit to the present data for the 2^+ state at 1·37 MeV and the result is shown in figure 15. The fit is excellent for θ = 28·6°.

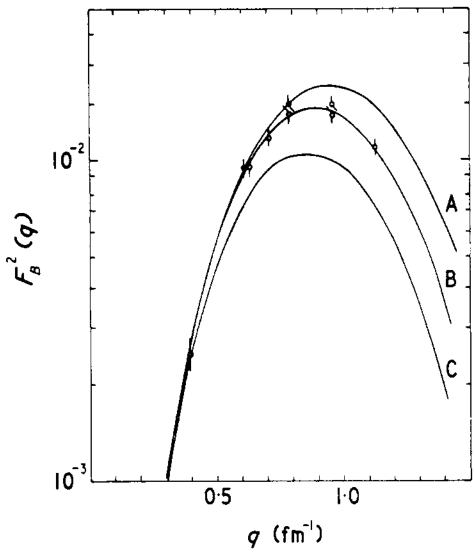

Figure 15. Comparison of $F_B^2(q)$ for the 1·37 MeV (2^+) state with: A, Hartree–Fock; B, CAP; and C, Nilsson model calculations.

The remaining form factors were then calculated with all parameters fixed and the results are shown in figure 16 and 17 for the K = 2, $J^\pi = 2^+$ and $J^\pi = 4^+$ states respectively. No agreement is obtained for the 2^+ state, the radial dependence and the magnitude both being wrong. Hauge *et al* (1971) note that the asymmetry parameter γ is important for the 2^+ state and show that reasonable agreement is obtained for γ = 10°. Thus these results imply an asymmetric shape for ^{24}Mg. The CAP model results for the 4^+ state in figure 17 are in fair agreement with experiment in both magnitude and q dependence. The calculated form factors for the K = 0, $J^\pi = 4^+$ state at 4·12 MeV are shown in figure 16 together with the data for the 2^+ state at 4·23 MeV since these states could not have been resolved experimentally. It can be seen from this diagram that a 4^+ state of this strength could not have been observed since the cross section of the 2^+ state dominates at all values of momentum transfer used in the present experiment.

The K = 2 band based on the first excited vibrational state at 6·43 MeV is of some interest. Hauge *et al* (1971) identify the base member of the K = 2 band with the 2^+ state at 8·7 MeV, but this state was not observed in the present experiment. The 2^+

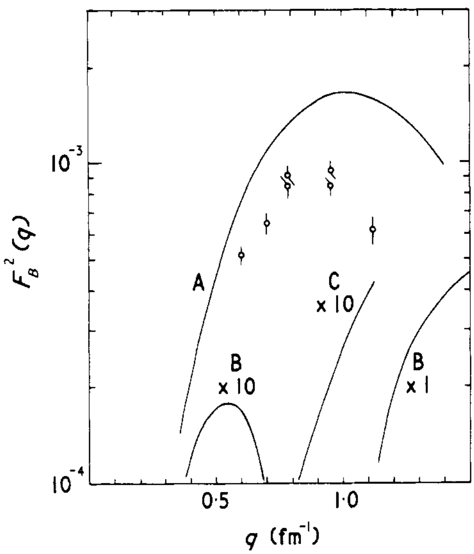

Figure 16. Comparison of $F_B^2(q)$ for the 4·23 MeV (2^+) state with: A, Hartree–Fock; and B, CAP calculations. The CAP model prediction for the 4^+ state at 4·12 MeV is shown as curve C.

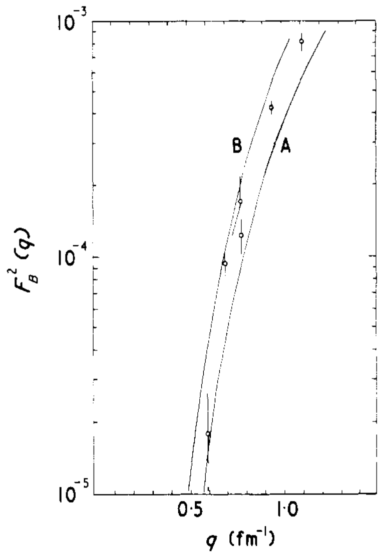

Figure 17. Comparison of $F_B^2(q)$ for the 6·00 MeV (4^+) state with: A, Hartree–Fock; and B, CAP predictions.

state at 9·30 MeV is, however, quite close to the predicted energy and could be the $K = 2$ state. The CAP model prediction for the 4^+ member of this band is at 10·3 MeV and, therefore, coincides almost precisely with the state at 10·35 MeV observed in this experiment and to which the spin and parity of 4^+ have been assigned. The form factors for these levels are not readily calculable but one can check on internal consistency by comparing the relative strengths of these transitions with those of the $K = 2$ band based on the ground state vibration. The following results are obtained:

$$\frac{B(\mathrm{E4}; 0^+ \to 4^+, \omega_0, K = 2)}{B(\mathrm{E2}; 0^+ \to 2^+, \omega_0, K = 2)} = (1{\cdot}4 \pm 0{\cdot}4) \times 10^3\ \mathrm{fm}^4$$

and

$$\frac{B(\mathrm{E4}; 0^+ \to 4^+, \omega_1, K = 2)}{B(\mathrm{E2}; 0^+ \to 2^+, \omega_1, K = 2)} = (1{\cdot}0 \pm 0{\cdot}4) \times 10^3\ \mathrm{fm}^4.$$

Here ω_0, and ω_1 indicate the ground and first excited vibrations respectively. Since the contribution of the vibrational parts of the wavefunctions is the only difference between the two bands and since this contribution is effectively equalized in taking these ratios one would expect the results to be identical if the CAP model description of these states is correct. The above results, therefore, give support to the CAP model description of these states.

Another recent verification of the predicted spectrum of the CAP model (see Hauge *et al* 1971) is the observation by Branford *et al* (1971) of a $J^\pi = 5^-$ state at 10·03 MeV which was found to be a member of a $K^\pi = 0^-$ band, the lower members being the 7·56 MeV 1^- and 8·36 MeV 3^- states. These are the assignments of the CAP model.

It can be concluded that the alpha particle model of ^{24}Mg in the form of an asymmetric bitetrahedron of six α-clusters gives a fair description of the low-lying states of ^{24}Mg.

6.2. *The Nilsson model*

The Nilsson model (Nilsson 1955) has met with some considerable success in applications to deformed nuclei in the region of $A = 25$. For this reason we have used an extended Nilsson model which includes all orbitals in the first seven major shells and applied the technique to ^{24}Mg. The resulting minimum energy of the nucleus was obtained for $\eta = 4{\cdot}5$, η being Nilsson's deformation parameter. The value of the oscillator parameter was determined from elastic electron scattering and was found to be $b = 1{\cdot}76$ fm.

The form factors for the excitation of the $K = 0, J^\pi = 2^+$ state by electron scattering were calculated and the results are compared to the data in figure 15, where it can be seen that the calculation underestimates the cross section by about 30%. There are, however, no variable parameters in this calculation whereas the CAP model has θ as a parameter and the Hartree–Fock calculations (to be discussed in § 6.3) include effective charge. The improvement of the Nilsson model calculation over the Hartree–Fock results without effective charge is undoubtedly due to the inclusion of the contributions of higher shells.

6.3. *Projected Hartree–Fock calculations for ^{24}Mg*

The lowest Hartree–Fock (HF) solution for ^{24}Mg found by Bar Touv and Kelson (1965) had triaxial symmetry. This was obtained by considering ^{24}Mg as an inert ^{16}O core plus eight particles in the s–d shell, and the resulting reduced transition probability for the excitation of the first excited state was $75e^2$ fm^4. This low result is characteristic of all such inert core calculations and it has become common practice (Wilkinson 1967) to introduce an effective charge of $\epsilon = 0{\cdot}5e$ for both neutrons and protons to simulate the effects of the core. Many other solutions have since been found including the cubic (Glen and MacDonald 1971), tetragonal, and axial symmetries (Watt 1971). The cubic solution is interesting in that it is the only result which predicts a 0^+ state in the vicinity of the observed state at 6·43 MeV.

Watt (1972, private communication) has calculated the electron scattering form factors for the excitation of the low-lying states of ^{24}Mg and these are compared to the result of the present experiment in figures 15, 16, 17 and 18 for the 1·37 MeV (2^+),

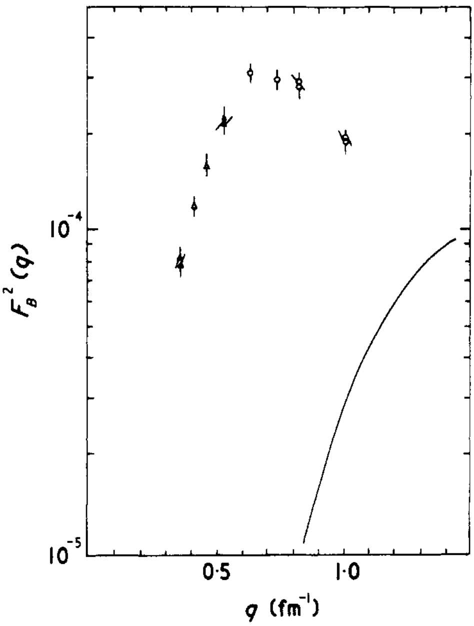

Figure 18. Comparison of $F_B^2(q)$ for the 6·43 MeV (0^+) state with the Hartree–Fock calculation.

4·23 MeV (2^+), 6·00 MeV (4^+) and 6·43 MeV (0^+) states respectively. An effective charge of $0{\cdot}5e$ has been assumed throughout. The predictions for the 2^+ state at 1·37 MeV are in good agreement with experiment at low q but at higher q values the deviations are more marked. The calculation for the second 2^+ state at 4·23 MeV are not in such good agreement but it is significant that the HF result is substantially better than the CAP model result for the axially symmetric case. Since the major contribution to the HF wavefunctions arises from the triaxial solution this result is further evidence for the non-axial symmetry of ^{24}Mg. The HF result for the $K = 2$, $J^\pi = 4^+$ state at 6·00 MeV is in fair agreement with experiment, and the predictions for the $K = 0$, $J^\pi = 4^+$ state are so much lower than the data for the 2^+ state at 4·23 MeV that no conclusions can be drawn. The most serious disagreement with experiment occurs for the 0^+ state of the cubic solution, shown in figure 18. For this state the dependence on momentum transfer and the magnitude are both wrong and this is probably due to the restriction of the orbitals to the s–d shell basis.

There have been several HF calculations in which a larger basis has been employed, the most extensive being that by Cusson and Lee (1973) in which all orbitals in the first five major oscillator shells were included. The result was a non-axial solution which predicts, without the necessity of effective charge, electromagnetic matrix elements which are in good agreement with experiment. For example, the result for the $B(\text{E2}, \uparrow)$ value for the first excited state is $B(\text{E2}) = 392e^2\ \text{fm}^4$, compared to the present results of

$$B(\text{E2}) = (416 \pm 25)e^2\ \text{fm}^4.$$

6.4. The $T = 1$ states of ^{24}Mg

Considerable evidence has been accrued from stripping reactions which has enabled the identification of the $T = 1$ states of ^{24}Mg. The five lowest such states were identified by Lawergren *et al* (1968) at 9·52 MeV (4^+), 9·98 MeV (1^+), 10·07 MeV (2^+), 10·74 MeV (1^+) and 11·22 MeV. Tang *et al* (1969) provided the $T = 1$ identification for the states at 12·53 MeV (1^+) and 12·67 MeV (2^-). In addition, a tentative assignment of $T = 1$ to a 2^- state at 13·37 MeV was made by Fagg *et al* (1970) using inelastic electron scattering at 180°. Of the states mentioned above the present experiment observed those at 9·98, 10·74, 12·67 and 13·37 MeV. In addition two 2^+ states were observed at 12·52 and 12·99 MeV, both of which possess large transverse contributions to their cross sections and which may be isobaric analogue states.

The 1^+ states at 9·97 and 10·74 MeV may be due to a $\text{d}\frac{5}{2} \to \text{d}\frac{3}{2}$ spin-flip transition. A proper shell model calculation of the energies and wavefunctions of such states is an extensive calculation for ^{24}Mg but one can easily obtain the q dependence of the electron scattering form factors from the relevant s–d shell matrix elements given, for example, by Willey (1963). The form factors for these states then become

$$F(q) = ky^{1/2}\,\text{e}^{-y}(8{\cdot}4 - 9{\cdot}44y - 1{\cdot}88y^2)\phi(q)$$

where $y = b^2q^2/4$, b is the oscillator parameter and k is an arbitrary normalization factor. $\phi(q)$ takes into account the finite nucleon size and the motion of the centre of mass. The results obtained using this expression with an oscillator parameter of $b = 1{\cdot}60$ fm are compared with the data in figure 19 where it can be seen that a good fit is obtained. A similar calculation for the transition $2\text{s}\frac{1}{2} \to 1\text{d}\frac{3}{2}$ cannot fit the experimental data for any reasonable value of b as is shown in figure 19. These straightforward considerations thus identify the origin of the $T = 1$, $J^\pi = 1^+$ states.

Of the two $J^\pi = 2^-$ states observed in the present experiment only the 12·67 MeV state has been identified as having $T = 1$ from stripping reaction studies. The strength of the observed transition to the 13·37 MeV state certainly indicates the $T = 1$ assignment but it is of interest to see whether the isospin dependence of the multipole operators can enable an assignment on the basis of the q dependence of the transition. The lowest energy single particle transition which would give rise to a 2^- state is the $1\text{p}\frac{1}{2} \to 1\text{d}\frac{5}{2}$ transition and we have evaluated the form factors for this transition on the basis of a $\Delta T = 1$ and $\Delta T = 0$ transition. The former case was used to fit the 12·67 MeV transition as shown in figure 20 and the oscillator parameter required was $b = 1{\cdot}65$ fm in close agreement with the result obtained for the M1 transitions. This value was then used to compare the 13·37 MeV data with the $T = 0$ and $T = 1$ assignments. The results shown in figure 21 favour the $T = 1$ assignment but higher momentum transfer data would be

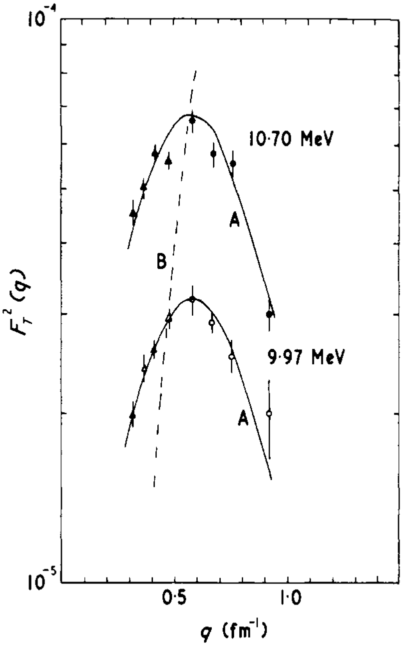

Figure 19. Comparison of $F_T^2(q)$ for the 1^+ states at 9·97 MeV and 10·70 MeV with the q dependence of the single particle transitions: A, $1d\frac{5}{2} \rightarrow 1d\frac{3}{2}$; and B, $2s\frac{1}{2} \rightarrow 1d\frac{3}{2}$.

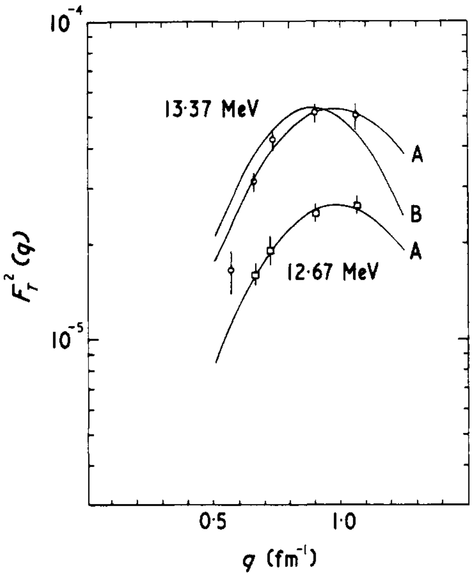

Figure 20. Comparison of $F_T^2(q)$ for the 2^- states at 12·67 MeV and 13·37 MeV with the q dependence of the $1p\frac{1}{2} \rightarrow 1d\frac{5}{2}$ transition for: A, $T = 1$; and B, $T = 0$.

more conclusive. Nevertheless, taken in conjunction with the strength of the transition this evidence strongly favours a $T = 1$ assignment for the 13·37 MeV state. It should be noted that each of the possible $p \rightarrow d$ transitions give similar results but the $1p\frac{3}{2} \rightarrow 2s\frac{1}{2}$ transition is excluded on the basis of the predicted q dependence.

The states excited at 12·52 and 12·99 MeV in the present experiment both have $J^\pi = 2^+$ and show large transverse contributions to the form factors. It is, therefore, possible that these states have isospin $T = 1$ and could correspond to the 2^+ member of the single particle $1d\frac{5}{2} \rightarrow 1d\frac{3}{2}$ transition.

As noted above, a $T = 1$ state with $J^\pi = 1^+$ has previously been observed at $E_x = 12{\cdot}53$ MeV in stripping reactions but this state is not excited in the present experiment because the 1^+ states at 9·97 and 10·7 MeV contain most of the M1 strength for ^{24}Mg. Tang *et al* (1969), however, observed an $l_p = 2$ stripping pattern in the ^{23}Na(d, n)^{24}Mg reaction at this excitation energy in addition to the $l_p = 0$ pattern corresponding to the population of the 1^+ state. This supports the present observation of a 2^+ state at this energy. The ^{23}Na(d, p)^{24}Na reaction (Daum 1963) also shows both $l_n = 0$ and $l_n = 2$ stripping patterns at 12·52 MeV and the relative spectroscopic factor for the $l = 2$ components in the two reactions is consistent with the values obtained for the other $T = 1$ states. In addition, the α width for this energy is small. These results together with the present data suggest the existence of a $T = 1, 2^+$ state at this energy. The stripping reaction experiments did not, however, investigate the 13·0 MeV region. Calculations of the transverse form factors for these states based on the $1d\frac{5}{2} \rightarrow 1d\frac{3}{2}$ single particle transition can only be constrained to fit the data for the rather large oscillator parameter of $b = 2{\cdot}1$ fm. It would appear, therefore, that a more complex configuration must be invoked to explain the q dependence of these transitions.

7. Conclusions

The present work has confirmed the results of Titze (1969) for the ground state reduced transition probabilities and transition radii of the states at 1·37 MeV (2^+), 4·23 MeV (2^+), 6·43 MeV (0^+) and 9·30 MeV (2^+), and has extended the cross section measurements to higher values of momentum transfer. The result for the 6·00 MeV (4^+) state confirms the (e, e') work of Junk (1970) rather than the (α, α') result of Naqib and Blair (1968). The data for the 3^- states at 7·59 and 8·36 MeV agree with the results of Titze (1969) but the B(E3) values obtained are reduced by the DWBA analysis.

The ground state widths deduced from the present work for the 1^+ states at 9·97 and 10·70 MeV are lower than the previous measurements by (e, e') at 180° and (γ, γ'). The (γ, γ') results have been explained but the discrepancy with the previous (e, e') measurement remains. The measured cross sections for the transition at 10·35 MeV indicate the presence of a 4^+ state in addition to the known 2^+ state and it has been shown that some evidence for the existence of such a doublet already exists from studies of the ^{23}Na(d, n)^{24}Mg reaction.

In the complex region of the excitation spectra between 11·0 and 14·0 MeV many transitions have been observed and identified. In particular the $J^\pi = 2^-, T = 1$ state at 12·67 MeV has been observed by electron scattering for the first time and the deduced ground state width is in good agreement with that obtained from the ^{23}Na(p, γ)^{24}Mg reaction. The 2^- assignment of Fagg *et al* (1970) to the transition observed at 13·37 MeV has been confirmed but the deduced ground state width is somewhat lower than the previous measurement. It has been shown, however, that the present result is in good agreement with the (p, γ) work if the assignment of $J^\pi = 2^-, T = 1$ is made to the resonance observed by Mayer *et al* (1972) at 13·365 MeV.

Comparison of the experimental form factors for the low-lying states with the predictions of nuclear models has shown that the classical alpha particle model provides a fair description of the structure of ^{24}Mg. The main deficiencies in the form factors deduced from the Hartree–Fock calculations have been shown to arise from the restriction of the basis to the s–d shell and the more recent calculations of Cusson and Lee (1973) have overcome this restriction and reproduce the experimental data very well. For the higher excitation energy transitions it has been shown that the M1 transitions at 9·97 and 10·70 MeV and the M2 transitions at 12·67 and 13·37 MeV can be understood in terms of simple single particle shell model transitions.

Acknowledgments

The authors would like to thank the UK Science Research Council for their financial support of this work. Much help was given in the development of computer programs for the data analysis and in the data collection by S W Brain, C S Curran, E W Lees and R P Singhal, and this is gratefully acknowledged. We also thank the other stalwarts who assisted in the data collection, D M Fleming, W A Gillespie and A G Slight. Dr I F Wright and Dr A Watt are thanked for the communication of their results and permission to use them before publication. Finally, we express our gratitude to Professor G R Bishop for his interest and encouragement throughout the period of research on this project.

References

Anderson J A and Ritter R C 1969 *Nucl. Phys.* A **128** 305–24
Bar-Touv J and Kelson I 1965 *Phys. Rev.* **138** B1035
Bergstrom J C 1967 *MIT Summer Study Report No.* TID-24667 pp 251–64
Branford D *et al* 1971 *Phys. Lett.* **36B** 456
Chertock B T *et al* 1970 *Phys. Rev.* C **2** 2028–30
Cline D and Lesser P M S 1970 *Nucl. Instrum. Meth.* **82** 291–3
Crawley G M and Garvey G T 1967 *Phys. Rev.* **160** 981–96
Curran C S *et al* 1972 *J. Phys.* A: *Gen. Phys.* **5** L39–42
Cusson R Y and Lee H C 1973 *Nucl. Phys.* A **211** 429–62
Daum C 1963 *Nucl. Phys.* **45** 273
Drechsel D 1968 *Nucl. Phys.* A **113** 665–75
Eisenberg J M and Rose M E 1963 *Phys. Rev.* **131** 848
Endt P M and Van der Leun C 1967 *Nucl. Phys.* A **105** 1–488
Fagg L W *et al* 1970 *Phys. Rev.* C **1** 1137–8
de Forest T and Walecka J D 1966 *Adv. Phys.* **15** 1–109
Fuchs H *et al* 1968 *Nucl. Phys.* A **122** 59–72
Glen J A and MacDonald N 1971 *Nucl. Phys.* A **165** 524–32
Goldberg E *et al* 1954 *Phys. Rev.* **93** 799–805
Hauge P S *et al* 1971 *Phys. Rev.* C **4** 1044–61
Häusser O *et al* 1970 *Can. J. Phys.* **48** 35–45
Helm R H 1956 *Phys. Rev.* **104** 1466–75
Herrmann D and Kalus J 1970 *Nucl. Phys.* A **140** 257–60
Highland G J and Thwaites T T 1968 *Nucl. Phys.* A **109** 163–76
Hogg G R *et al* 1972 *Nucl. Instrum. Meth.* **101** 203–19
Horowitz Y S *et al* 1969 *Nucl. Phys.* A **134** 577–98
Junk P 1970 *PhD Thesis* University of Mainz
Kuehne H W, Axel P and Sutton D C 1967 *Phys. Rev.* **163** 1278–91
Lawergren B T *et al* 1968 *Nucl. Phys.* A **108** 325–36
Lawergren B T *et al* 1970 *Phys. Rev.* C **1** 994–9
Maximon L C 1969 *Rev. mod. Phys.* **41** 193–204

Maximon L C and Isabelle D B 1964 *Phys. Rev.* **136** B674–83
Mayer M A *et al* 1972 *Nucl. Phys.* A **185** 625–43
Nakada A and Torizuka Y 1972 *J. Phys. Soc. Japan* **32** 1–13
Naqib I M and Blair J S 1968 *Phys. Rev.* **165** 1250–63
Nilsson S G 1955 *K. Danske Vidensk Selsk., Math.-fys. Meddr* No 16
Penner S 1961 *Design of a High Resolution, Moderate Solid Angle Spectrometer for High Energy Electron Scattering NBS Internal Report*
Powell M J D 1964 *Comput. J.* 7 155–62
Rawitscher G H and Fischer C R 1961 *Phys. Rev.* **122** 1330–7
Robinson S W and Bent R D 1968 *Phys. Rev.* **168** 1266–86
Rosen M *et al* 1967 *Phys. Rev.* **163** 927–34
Schucan T H 1968 *Phys. Rev.* **171** 1142–50
Singhal R P *et al* 1974 *Nucl. Phys.* A **218** 189–200
Stark W J *et al* 1970 *Phys. Rev.* C **1** 1752–6
Swann C P 1971 *Phys. Rev.* C **4** 1489–90
Tang S M *et al* 1969 *Nucl. Phys.* A **125** 289–304
Tassie L J 1956 *Aust. J. Phys.* **9** 407–18
Titze O 1969 *Z. Phys.* **220** 66–85
Toepffer C and Drechsel D 1968 *Z. Phys.* **210** 423–33
Torizuka Y *et al* 1969 *Phys. Rev. Lett.* **22** 544–6
Tuan S T *et al* 1968 *Nucl. Instrum. Meth.* **60** 70–6
Vitoux D *et al* 1970 *Phys. Rev.* C **3** 718–24
Walecka J D 1962 *Phys. Rev.* **126** 653–62
Watt A 1971 *Nucl. Phys.* A **172** 260–72
Wilkinson D H 1967 *Comments Nucl. Part. Phys.* **1** 139
Willey R S 1963 *Nucl. Phys.* **40** 529–65